CFD Validation of Hydrofoil Performance Characteristics in Cavitating and Non-Cavitating Flows

Tristan L. Wood

B. Eng. Mechanical Engineering
Project Report
Department of Mechanical Engineering
Curtin University

2013

[This page has been left intentionally blank]

Mandurah
WA 6210

08th November 2013

The Head
Department of Mechanical Engineering,
Curtin University,
Kent Street,
Bentley,
WA 6102

Dear Sir:

I submit this report entitled "CFD Validation of Hydrofoil Performance Characteristics in Cavitating and Non-Cavitating Flows", based on Mechanical Project 491/493, undertaken by me as part-requirement for the degree of B.Eng. in Mechanical Engineering.

Yours faithfully,

Tristan L. Wood

[This page has been left intentionally blank]

Acknowledgements

Foremost, I would like to express my sincere gratitude to my primary supervisor, Doctor Andrew King for his continuous support of my final year project, for his patience, enthusiasm and immense technical knowledge in the area of computational fluid dynamics and the openFOAM open source CFD software, all of which have been deeply appreciated.

I would similarly like to thank Doctor Tim Gourlay, Senior Research Fellow with the Center for Marine Science and technology for his support and enthusiasm in this project and his provision of data and technical materials used for the completion of this project.

In addition I would like to acknowledge that this work was supported by Pawsey funded iVEC through the use of advanced computing resources located at the iVEC@murdoch facility by the use of their Epic HP Linux Cluster used to complete CFD simulations that would have been impractical to achieve with standard computing systems in the allotted time.

Finally I would like to thank my fellow Engineering Final Year students who have provided both support and general advice for the duration of this project.

[This page has been left intentionally blank]

Abstract

This study attempts to validate the use of an open source CFD package, OpenFOAM to assess the performance characteristics of a hydrofoil in both sub-cavitating and fully cavitating flows and compare these to known performance characteristics for such a design obtained previously using experimental methods. A symmetrical NACA 66-012 section hydrofoil was selected and its performance characteristics including parameters such as lift and drag coefficients and quarter chord pitching moments were calculated for a range of flow velocity's and angles of attack in sub-cavitating flow and at a constant angle of attack with varying cavitation numbers in cavitating flows, following this the results were compared to the known data.

Results gained from the sub-cavitating simulations shows that the forces experienced on a hydrofoil could be predicted to within a consistent 10-15% variance from the experimental data published by Keerman in 1956. In the case of the cavitating flow simulations showed large variances of up to 75% between the experimental and the CFD data. Whilst this variance would be considered large for such work according to work published by Gosset in 2010 notes that for a simulation using the OpenFOAM solver model selected on a symmetrical hydrofoil that results within an order of magnitude are acceptable.

Thus the knowledge gained from this study shows that the accuracy of the data gained using CFD techniques to predict the performance characteristics of hydrofoils are highly dependent on the complexity and design of modelling system used and the quantity of computational processing power available.

Nomenclature

1. 'A' Plan form area of hydrofoil (m^2)
2. 'α' Hydrofoil angle of Attack (°)
3. 'c' Chord length of hydrofoil (m)
4. 'C_L' Coefficient of Lift
5. 'C_D' Coefficient of Drag
6. 'C_M' Quarter Chord Pitching Moment
7. 'C_P' Pressure Coefficient
8. 'D' Drag force on hydrofoil (N)
9. 'η' Performance ratio of hydrofoil
10. *'g'* Acceleration due to gravity (m/s^2)
11. *'k'* Cavitation number
12. *'L'* Lift force on hydrofoil (N)
13. *'M'* Moment acting at quarter chord on hydrofoil (N.m)
14. *'μ'* Dynamic Viscosity of water ($N.s/m^2$)
15. *'p'* Fluid Pressure (Pa)
16. *'p_∞'* Free stream fluid Pressure (Pa)
17. *'p_v'* Vapor pressure of fluid (Pa)
18. *'Pr'* Prandtl Number
19. *'Re'* Reynolds Number for fluid flows (Dimensionless Quantity)
20. *'ρ'* Density of water in bed apparatus (kg/m^3)
21. *'q'* Dynamic Pressure (velocity Pressure) of flow (Pa)
22. *'S_p'* Specific area of packing material (m^2/m^3)
23. *'U'* Flow velocity of fluid in the bed apparatus (m/s)
24. *'t '* Time component (s)
25. *'τ'* Shear stress (Pa)
26. *'u'* Velocity component in x axis (m/s)
27. *'v'* Velocity component in y axis (m/s)
28. *'v'* Kinematic viscosity of fluid (m^2/s)
29. *'w'* Velocity component in z axis (m/s)
30. 'x' Spatial Ordinate

31. ‘*y*’ Spatial Ordinate

32. ‘*z*’ Spatial Ordinate

Abbreviations

CFD	-	Computational Fluid Dynamics
RANS	-	Reynolds Averaged Navier-Stokes
LES	-	Large Eddy Simulation
DNS	-	Direct Numerical Simulation
NACA	-	National Advisory Committee on Aeronautics
STL	-	STereoLithography
VOF	-	Volume of Fluid
OpenFOAM	-	Open Field Operation And Manipulation
CAD	-	Computer Aided Design
FVM	-	Finite Volume Method
SST	-	Shear Stress Tensor
RMS	-	Root Mean Squared

Table of Contents

Page Number

List of Figures

Page Number

List of Tables

1.0 Introduction

The basic principle of standard hydrofoil craft is to raise a ships hull from the water and support it dynamically on a wing like foil lifting surface. The effect of lifting a ships hull from the water include the reduction of wave effects on the ship resulting in a smother ride as well as a decrease in power required to maintain modestly high cruising speeds as the hull no longer suffers drag effects from the water. Historically when designing hydrofoil craft, engineers and marine architects have relied on empirical methods and data for the selection of hydrofoil sections followed by costly and time consuming experimental testing of scale and full sized models.

Currently hydrodynamic data is widely available for a large range of standardized geometric shapes such as wedges, plates and circular arc hydrofoils as well as conventional cambered airfoil shapes. Symmetrical hydrofoil shapes have traditionally played important roles as both lifting surfaces and non-lifting support struts and fairings as the requirements for such structures including drag profiles and strength requirements are very similar to lifting hydrofoils.

Estimates place a theoretical weight limit of somewhere in the vicinity of 400 tones displacement for practical designs of hydrofoil craft using current hydrofoil technology (Pike, J. 2011). This limit is an application of the square-cube rule where the lift generated by a hydrofoil is proportional to its planform area, whilst the weight that each foil must support is proportional to volume or linear dimension cubed. Thus above this limit the foils tend to outgrow the hull dimensions and result in a number of impracticalities that render such designs unsuitable for commercial uses. In aircraft design such a problem would be countered by increasing wing loading or operational speeds, however in hydrofoil craft this is generally not an option as practical hydrofoil speeds are limited by cavitation effects.

Thus to continue the development of heavier and higher speed hydrofoil craft new and novel designs are required for hydrofoils that may include highly asymmetrical super-

cavitating or base vented foils or even multi component foils with variable geometries for operating over a range of speeds.

The development of said advanced hydrofoil designs using traditional experimental methods would be both time consuming and exorbitantly expensive, however by using CFD techniques this process can be optimized to reduce both time and costs with experimental testing required only at the final phase to confirm the performance characteristics of a hydrofoil designed using these practices. Unfortunately as a result of poor performance in the earlier years of development, naval architects and engineers tend to express an inherent distrust in CFD and the data it provides. Due to this there is a need for continual development of CFD techniques and technologies and for engineers in this field to confirm that accurate data can be practically produced using such methods.

This study attempts to validate the use of an open source CFD package, OpenFOAM to assess the performance characteristics of a hydrofoil in both sub-cavitating and fully cavitating flows and compare these to known performance characteristics for such a design obtained previously using experimental methods.

To begin this project the first requirement was to select a foil design to test. The selected foil for this project was a (National Advisory Committee on Aeronautics) NACA66-012 profile foil. The reason for the selection of this foil was that it is a symmetrical foil of a type commonly used for lifting bodies, control surfaces and supporting struts also as most foils are only operated with angles of attack between 0 and 15 degrees selection of a symmetrical foil limits the number of simulations required to understand the performance of the foil for each flow condition as performance will be comparable with both positive and negative angles of attack. Additionally there was a large quantity of data available on the performance characteristics of this foil in both sub-cavitating flows and cavitating flows at a range of flow velocities and angles of attack.

Design of the model of the foil was carried out using data from the National Advisory Committee on Aeronautics database of foil designs and was modelled using Dassault systems Soildworks to create a three dimensional model of the foil used by Keerman for his experimental testing. Following this a STereoLithography model of the foil was created from the Solidworks design. This model was created as this open source format allows for the inbuilt meshing tools in OpenFOAM to create a mesh around the foil.

Following this a suitable domain was selected to both allow for modelling of effects upstream of the foil and those downstream in the wake of the foil. With the model and domain defined and the boundary conditions set simulations were carried out for sub cavitating flow conditions using OpenFOAM's simpleFoam solver for a range of flow velocities ranging from 9.45 meters per second to 17.5 meters per second. For these flows the foil was adjusted from angles of attack of 0 through to a maximum of +13 degrees in one-degree increments. SimpleFoam is a steady state solver inbuilt into OpenFOAM for solving incompressible flows with turbulence modelling. Results for lift and drag forces as well as quarter chord pitching moments were recorded and then compared to those predicted by the experimental data published by Keerman.

Forces acting on the hydrofoil were obtained by integrating the pressure acting upon the hydrofoil and then resolving the resultant force into forces in the directions normal and parallel to the flow to determine the lift and drag forces. The coefficients of lift and drag were the determined by Appling these forces to the lift and drag equations which accounts for the free stream dynamic pressure and plan form area of the foil.

Simulation of the cavitating flow conditions were carried out in a similar manner to the non-cavitating flow conditions with several exceptions. Rather than adjusting the flow velocity and angle of attack a constant flow velocity of 9.45 meters per section and angel of attack of 10 degrees were used and the cavitation number of the flow from a range of 0.220 to 5.4 was adjusted by altering the free stream pressure of the fluid. Additionally a multi-phase solver from OpenFOAM, inetrPhaseChangeFoam was used in place of simpleFoam. This solver is a model based on solving for 2 incompressible,

isothermal immiscible fluids with phase-change (e.g. cavitation) using a VOF (volume of fluid) phase-fraction based interface capturing approach. As in the sub-cavitating case the forces acting on the foil were determined by integration of pressure and the coefficients of lift and drag were calculated in the same manner. The resulting forces were also compared to those predicted by Keerman and in addition the hydrofoil performance ratios (ratio of lift to drag) were calculated and also compared.

Simulation of the sub-cavitating cases took approximately 70-80 CPU hours to complete with the results showing an interesting series of trends. Analyses of the determined coefficients of both lift and drag in the sub-cavitating case shows that the simpleFoam model tends to over predict the forces acting on the hydrofoil. In all cases the resultant forces were over predicted, usually by approximately 10% but in some cases a number of points were as far as 25% above predicted results. However the model also tended to over predict the drag forces by an amount greater than the lift forces. This resulted in the hydrofoil performance ratio (lift to drag ratio) being consistently less than what was predicted by Keerman.

Simulation of the cavitating flows was a much more computationally intensive process requiring the use of iVEC's supercomputing facilities to complete in a timely manner, as each case required approximately 700-800 CPU hours to resolve. In this case the results did not follow an obvious trend as was seen in the previous cases. For the lift forces experienced by the foil the results obtained for cavitation numbers of 1.5 through 3.5 showed a reasonable level of agreement within what would have been expected for such a simulation whilst at lover cavitation numbers the lift force produce was far greater than what was experimentally determined and at higher cavitation numbers the lift force calculated was slightly lower than experimental data predicted. The drag forces experienced by the foil also tended to show a large variance between the experimental and the computational results. For cavitation numbers between 1 and 3.3 the drag forces tended to be under predicted by between 50 and 75% and whilst outside this set of cavitation numbers the reverse is the case with the forces tending to be over predicted by as great a margin.

Whilst these variances would be considered quite large for experimental type work, analysis covered in (Gosset 2010) where a very similar type simulation was attempted shows that in the case of cavitating flows when using a solver such as interphaseChangeFoam that results of coefficients of lift and drag within an order of magnitude can be considered acceptable results.

There are a number of possible sources of error that could have contributed to the variances between the experimental data and that from the CFD simulations. For the sub-cavitating flows the use of the very basic simpleFoam solver model that does not allow for compressibility of the fluid could have contributed to the error in the results. Additionally turbulence modelling on the surface of the hydrofoil using the RANS two equation k-ω SST model could have also contributed. Whist RANS turbulence modelling is one of the least processor intensive model schemes it is known to produce poor results in comparison to a more advanced turbulence model such as LES and is this considered to be among “the best of the worst”.

In the case of the cavitating flow simulations there were also a number of possible sources of error. Firstly cavitation is a complex phenomenon and there are a large variation in methods for modelling its effects such as models based on barotropic equations of state or like the model used base on the transport equation of vapour fractions. The result of using different modelling methods is that some work only in specific styles of simulations and thus the selection of the most suitable model is important in producing accurate results. Additionally in order to save computational power in already computationally intensive simulations turbulence was modelled using a laminar model scheme, which could have also resulted in potential errors in the results.

1.1 Project Objectives

There were a number of objectives for this project including

1. The first objective was to develop a working understanding of the open source OpenFoam computational fluid dynamics software in the Ubuntu operating environment then using this knowledge construct a series of CFD cases for determining the performance characteristics of a NACA66-012 hydrofoil.

2. Determine the performance characteristics including coefficient of lift and drag as well as the quarter chord pitching moments for NACA66-012 hydrofoil in sub-cavitating flows for flow velocities ranging from 9.45m/s to 17.5 m/s and angles of attack from 0-13°

3. Determine the performance characteristics including coefficient of lift and drag as well as the quarter chord pitching moments for NACA66-012 hydrofoil in incipient cavitation and fully developed cavitation flows for cavitation numbers ranging from 0.220 to 5.337 for a flow velocity of 9.45 m/s and angle of attack of 10°

1.2 Scope and Limitations of Theoretical Data Produced

1. The simulation was designed to test the performance characteristics of a NACA66-012 hydrofoil in a range of flow conditions and thus the hydrofoil model has a constant cross section and no supporting structure that would be required in real world applications of the foil and would therefore have interacting effects on the flow around the foil.
2. For sub-cavitating flows the use of the basic simpleFoam solver does not allow for compressibility or transient flows of the fluid in question. Whilst this is not a problem as the simulations were steady state and water is very nearly incompressible at the pressures in question, this solver is considered one of the most basic models available in the OpenFOAM package and fails to account for a number of fluid dynamics.
3. The Reynolds Averaged Navier Stokes (RANS) model used in the sub-cavitating simulations will only produce the average of the turbulent flow at each point rather than produce individual point data. This was used in order to reduce processing costs at the expense of accuracy.
4. The use of a laminar turbulence scheme for the cavitating flow simulations rather than a RANS scheme in order to save on processing power will result in a loss of accuracy in these simulations.
5. The use of the constant cross sectional foil that terminates at the front and rear boundary results in the flow effects that occur at the edge of the foil not being accounted for in the simulation.

[This Page Has Been Left Intentionally Blank]

2.0 Background

2.1 Theory

2.1.1 Navier-Stakes Equations

The cornerstones of CFD are the fundamental governing equations of fluid dynamics and are the continuity, momentum and energy equations. These equations are mathematical expressions of the three physical principles on which all fluid dynamics are based. To express these principles simply:

1. All mass, temperature and energy of a fluid are conserved
2. The momentum of each fluid particle is equal to the sum of the forces on a particle according to Newton's second law
3. The rate at which energy is gained or lost by the system or particle, shall always equal the sum of the rate of heat flow and the rate of work done on that system according to the first law of thermodynamics

Using the above three laws it is possie to describe the physical properties of a fluid element using a Cartesian coordinate system. The Navier-Stokes equations are a series of equations, which can be used to represent through mathematical expressions the combined influence of external factors on individual fluid elements. These equations were based on a Newtonian model of vicious stresses within a fluid medium and can be defined in three time dependent dimensions using a series of five partial differential equations.

Considering specifically at the conservation of mass for a finite element of fluid in a given system the following conservation of mass diagram can be constructed.

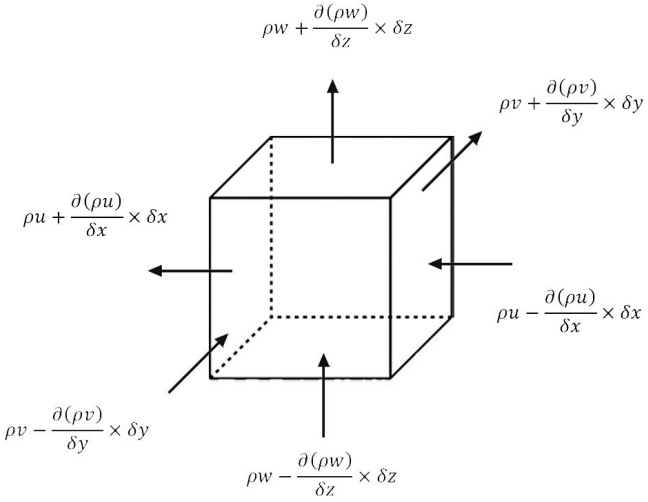

Figure 1: Fluid Element Subject to Forces According to Law of Conservation of Mass

This above diagram defines exclusively the mass flow rates of fluid entering and exiting the system without accounting for momentum changes and energy transfers involving the system. Taking this above system and arranging all terms of the resulting mass balance on the left hand side and dividing by the element volume δxδyδz yields.

$$\frac{\partial \rho}{\partial t} + \frac{\partial(\rho u)}{\partial x} + \frac{\partial(\rho v)}{\partial y} + \frac{\partial(\rho w)}{\partial z} = 0$$

Thus for a system utilizing an incompressible fluid with a fixed density such as that utilised by OpenFOAM's simpleFoam model the net mass flow rate of the element can be defined by the following equation where:

$$\frac{\partial u}{\partial x} + \frac{\partial v}{\partial x} + \frac{\partial w}{\partial x} = 0$$

Stating the above equation plainly "the rate of increase of a property per unit mass of fluid element and the net flow of the property per unit mass of fluid element are equal ate of increase of a property per unit mass for a fluid particle"

For the same fluid element the conservation of momentum can be defined by the flowing equation where:

$$\rho\left(\frac{\delta u}{\delta t}+u\frac{\delta u}{\delta x}+v\frac{\delta u}{\delta y}+w\frac{\delta u}{\delta z}\right)=Constant$$

The momentum equation in a specific Cartesian plane can be found by setting the rate of change of the momentum of the fluid element in a Cartesian axis equal to the total force in that axis on the element due to surface stresses plus the rate of increase of momentum in that axis due to external sources yielding the following equations:

The x-component of the momentum equation:

$$\rho\frac{Du}{Dt}=\frac{d(-p+\tau_{xx})}{dx}+\frac{d\tau_{yx}}{dy}+\frac{d\tau_{zx}}{dz}+S_{Mx}$$

The y-component of the momentum equation:

$$\rho\frac{Du}{Dt}=\frac{d(-p+\tau_{yy})}{dy}+\frac{d\tau_{xy}}{dx}+\frac{d\tau_{zy}}{dz}+S_{My}$$

The z-component of the momentum equation:

$$\rho\frac{Du}{Dt}=\frac{d(-p+\tau_{zz})}{dz}+\frac{d\tau_{yz}}{dy}+\frac{d\tau_{xz}}{dx}+S_{Mz}$$

For Newtonian fluids the governing equations contain as further unknowns the viscous stress components. In many fluid flows the viscous stresses acting on a fluid element can be expressed as functions of local deformation rates. In three-dimensional flows the local rate of deformation is composed of the linear deformation and volumetric deformation rates. The rate of linear deformation of a fluid element has a total of nine

components in all three dimensions, six of which are fully independent when the fluid in question exhibits isotropic behaviour (Schlichting, H 2000).

The three linear deformation components are defined by:

$$s_{xx} = \frac{du}{dx} \qquad s_{yy} = \frac{dv}{dy} \qquad s_{zz} = \frac{dw}{dz}$$

The six shearing linear deformation components are defined by:

$$s_{xy} = s_{yx} = \frac{1}{2}\left(\frac{du}{dy} + \frac{dv}{dx}\right) \; s_{yz} = s_{zy} = \frac{1}{2}\left(\frac{dv}{dz} + \frac{dw}{dy}\right) \; s_{xz} = s_{zx} = \frac{1}{2}\left(\frac{du}{dz} + \frac{dw}{dx}\right)$$

The volumetric deformation of the fluid element is defined by:

$$\frac{du}{dx} + \frac{dv}{dy} + \frac{dw}{dz} = div\, \boldsymbol{u}$$

For a Newtonian fluid, the viscous stresses are proportional to the rates of deformation. The three dimensional form of Newton's law of viscosity for flows of compressible fluids requires the use of two constants of proportionality. The first of these is the dynamic viscosity, μ, which is used for the relation of stresses to linear deformations and the second constant termed second viscosity, λ, used for the relation of stresses to volumetric deformation.

These nine viscous stress components may be described by the following relationships where:

$$\tau_{xx} = 2\mu\frac{du}{dx} + \lambda\, div\, \boldsymbol{u} \quad \tau_{yy} = 2\mu\frac{dv}{dy} + \lambda\, div\, \boldsymbol{u} \quad \tau_{zz} = 2\mu\frac{dw}{dz} + \lambda\, div\, \boldsymbol{u}$$

$$\tau_{xy} = \tau_{yx} = \mu\left(\frac{du}{dy} + \frac{dv}{dx}\right) \quad \tau_{xy} = \tau_{yx} = \mu\left(\frac{du}{dy} + \frac{dv}{dx}\right) \quad \tau_{xy} = \tau_{yx} = \mu\left(\frac{du}{dy} + \frac{dv}{dx}\right)$$

Substituting the above equations into the previously defined momentum equations yields the three momentum partial differential equations of Navier-Stokes equations. These equations were derived independently by English mathematician and physicist George G. Stokes and French engineer Claude-Louis Navier in the early 1800s. Navier-Stokes equations are in effect an extension of the previously defined Euler equations and serve to include the effects of viscosity on fluid flows. These equations are a set of five coupled differential equations that could in theory be solved using calculus techniques and defined by:

$$\frac{\partial \rho}{\partial t} + \frac{\partial (\rho u)}{\partial x} + \frac{\partial (\rho v)}{\partial y} + \frac{\partial (\rho w)}{\partial z} = 0$$

$$\frac{\partial (\rho u)}{\partial t} + \frac{\partial (\rho u^2)}{\partial x} + \frac{\partial (\rho uv)}{\partial y} + \frac{\partial (\rho uw)}{\partial z} = -\frac{\partial p}{\partial x} + \frac{1}{Re_r}\left[\frac{\partial \tau_{xx}}{\partial x} + \frac{\partial \tau_{xy}}{\partial y} + \frac{\partial \tau_{xz}}{\partial z}\right]$$

$$\frac{\partial (\rho v)}{\partial t} + \frac{\partial (\rho uv)}{\partial x} + \frac{\partial (\rho v^2)}{\partial y} + \frac{\partial (\rho vw)}{\partial z} = -\frac{\partial p}{\partial y} + \frac{1}{Re_r}\left[\frac{\partial \tau_{xy}}{\partial x} + \frac{\partial \tau_{yy}}{\partial y} + \frac{\partial \tau_{yz}}{\partial z}\right]$$

$$\frac{\partial (\rho w)}{\partial t} + \frac{\partial (\rho uw)}{\partial x} + \frac{\partial (\rho vw)}{\partial y} + \frac{\partial (\rho w^2)}{\partial z} = -\frac{\partial p}{\partial z} + \frac{1}{Re_r}\left[\frac{\partial \tau_{xz}}{\partial x} + \frac{\partial \tau_{yz}}{\partial y} + \frac{\partial \tau_{zz}}{\partial z}\right]$$

$$\begin{aligned}
&\frac{\partial (E_T)}{\partial t} + \frac{\partial (uE_T)}{\partial x} + \frac{\partial (vE_T)}{\partial y} + \frac{\partial (wE_T)}{\partial z} \\
&= -\frac{\partial (up)}{\partial x} - \frac{\partial (vp)}{\partial y} - \frac{\partial (wp)}{\partial z} - \frac{1}{Re_r . Pr_r}\left[\frac{\partial q_x}{\partial x} + \frac{\partial q_y}{\partial y} + \frac{\partial q_z}{\partial z}\right] \\
&+ \frac{1}{Re_r}\left[\frac{\partial}{\partial x}\left(u\tau_{xx} + v\tau_{xy} + w\tau_{xz}\right) + \frac{\partial}{\partial y}\left(u\tau_{xy} + v\tau_{yy} + w\tau_{yz}\right)\right. \\
&\left. + \frac{\partial}{\partial y}\left(u\tau_{xz} + v\tau_{yz} + w\tau_{zz}\right)\right]
\end{aligned}$$

2.1.2 Performance criteria of Hydrofoils

When determining the performance characteristics of a submerged body in a flow it is best to define the acting forces with respect to a flow fixed coordinate system with the origin at the midchord of the body (Jamieson, 1996). By integrating the pressure over the surface of the body the resultant normal force acting on the lifting body can be determined. Resolving this force into two components, one acting in the normal direction to the flow and one acting in line with the flow termed lift L, and drag D, forces respectively can be determined. Additionally a resultant moment M, will usually exist around the origin for most lifting bodies, by general rule of thumb this moment is taken to be positive when acting in the clockwise direction.

By taking these forces acting on the body a more useful performance criteria of a submerged body can be defined by relating these forces to the density of the fluid, flow velocity and a reference are for the body. These criterions are referred to as coefficients of lift, drag and moment, these components result in non dimensional quantities by dividing the forces and moment per unit span by the free stream dynamic pressure q, and for hydrofoils the chord length c, where:

$$q = \frac{\rho U_\infty^2}{2}$$

$$C_L = \frac{L}{\left(\frac{\rho U_\infty^2}{2}\right)A} \qquad C_D = \frac{D}{\left(\frac{\rho U_\infty^2}{2}\right)A} \qquad C_M = \frac{M}{\left(\frac{\rho U_\infty^2}{2}\right)A}$$

Note in the above equations the coefficients are based on a unit length of hydrofoil, thus in the case of a hydrofoil of a specific width the chord value would be replaced by the planform area A, defined as the multiple of the chord and span of the foil.

The hydrodynamic efficiency η, of a lifting body can be defined by the ratio of lift force to drag force acting on a foil, where:

$$\eta = \frac{L}{D} = \frac{C_L}{C_D}$$

As stated above the pitching moment on a foil is defined as the moment produced by the hydrodynamic force on a foil if that force is applied not to the center of pressure but at the aerodynamic center of the hydrofoil. It is worth noting that for symmetrical hydrofoils both the center of pressure and aerodynamic center occur at approximately 25% of the chord from the leading edge. For a foil if the lift force is imagined to act through the aerodynamic center the moment of the lift force changes in proportion to the fluid velocity squared. If the moment is divided by the dynamic pressure, area and chord of the foil the quarter chord pitching moment is defined. This value has importance in the design of hydrofoils as it quantifies a portion of the total moment on the foil that must be balanced. Thus the quarter chord pitching moment can be defined by:

$$C_Q = \frac{Pitching\ Moment}{\left(\frac{\rho U_\infty^2}{2}\right) A.c}$$

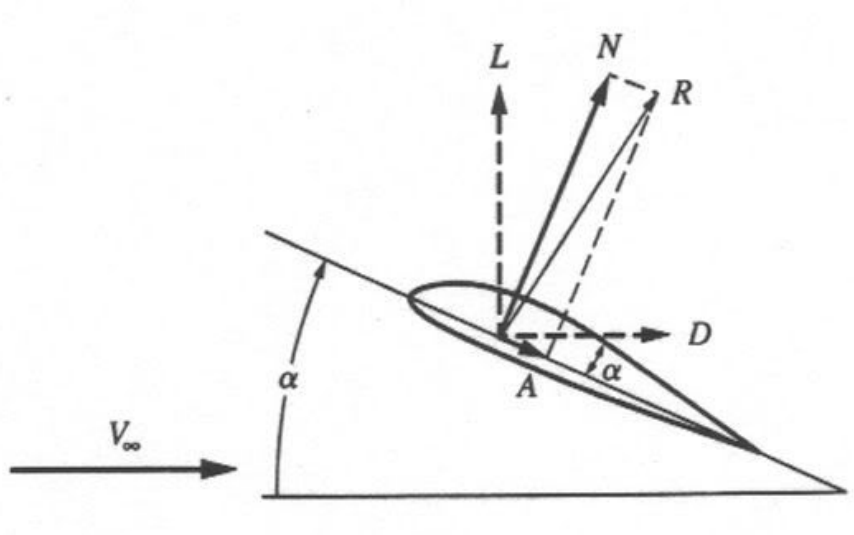

Figure 2: Diagram Depicting Forces Acting on Hydrofoil

2.1.3 Cavitation Effects on Hydrofoils and Lifting Surfaces

In a flow of liquid if the local pressure at a point falls below the vapor pressure of the fluid a phase change from liquid to vapor is likely to occur. This phase change from liquid to vapor due to this reduction in pressure is called cavitation. In order for this phenomenon to occur there is an additional requirement to a drop in pressure, this requirement is the inclusion of points of weakness in the form of small gas or vapor inclusions operating as initiation sites for breakdown of the liquid. These microbubbles within the fluid are termed cavitation nuclei and in the absence of such microbubbles it is possible for liquids to withstand negative absolute pressures in much the same way as solids. However in any practical application such weaknesses will occur in one of several forms.

Firstly thermal motions within a fluid will form temporary microscopic voids that will constitute the required nuclei necessary for rupture and growth of bubbles on a macroscopic scale. This form of nucleation is termed homogeneous nucleation and occurs spontaneously and randomly, without preferential nucleation sites. This form of nucleation is of little importance in the investigation of cavitation effects on lifting bodies.

The second form of nucleation is the more commonly observed manner that occurs when major weaknesses occur at the boundary between a liquid and a solid wall or small particles suspended within a liquid, where this happens with suspended particles it is usually difficult to distinguish from homogeneous nucleation. When rupture occurs at such sites it is termed heterogeneous nucleation, this form of nucleation is of much more interest when studying cavitation effects.

Another form of cavitation nucleation occurs when micron sized bubbles of contaminate gases, which may be attached to surfaces or within suspended particles or freely suspended within the liquid. In the case of water microbubbles of air will persist almost indefinitely and are almost impossible to remove outside of laboratory conditions. For

this reason the presence of such microbubbles tends to dominate most engineering applications.

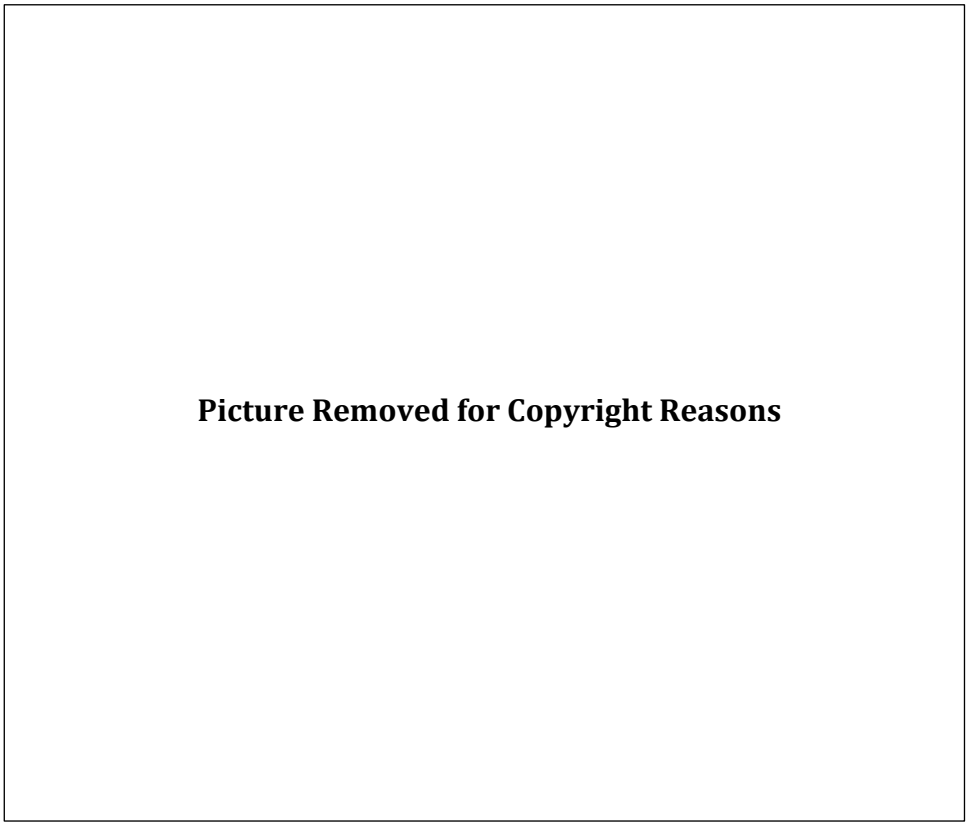

Figure 3: Modes of Heterogeneous Nucleation on Various Surface Conditions (Brennan 2003)

As seen in the above figure displaying heterogeneous forms of cavitation nucleation where contact angle between the vapor and solid intersection is denoted by θ. From this the tensile strength T, of the bubble surface in the case of the flat hydrophobic surface can be defined by:

$$T = 2S.\frac{\sin\theta}{R}$$

From this theoretically the tensile strength would tend to zero, as $\theta \rightarrow \pi$ radians. Alternatively the tensile strength on the hydrophilic surface is comparable with those of homogeneous nucleation situations with much higher tensile strengths.

Of course surfaces on the scale relevant to the nucleation of cavitation are not flat surfaces, so the effects of local geometry deformities must be considered (Brennan 2003). The case of the conical cavity in the above figure is often considered when attempting to exemplify the affects of surface geometry. From this example if the half angle of the vertex of such a cavity is denoted as α, then it is clear that a zero tensile strength situation occurs at a much more realizable value of:

$$\theta = \alpha + \frac{\pi}{2}$$

In addition should the value of θ be greater than defined in the above equation it is clear that such a vapor bubble would grow and fill the cavity at pressures above the vapor pressure for a liquid.

From this it is clear that surfaces will tend to have specific sites with optimum geometry's to promote nucleation of vapor bubbles and growth to macroscopic levels. It is also clear that as local pressures are reduced further more sites will become capable of generating and releasing vapor bubbles into the body of liquid.

The most common form of cavitation is though to occur in system where liquid flows where hydrodynamic effects result in regions around surfaces where the local pressure falls below vapor pressure of the fluid. The first person known to attempt to explain this unusual behavior seen most commonly around ships propellers when operating at high speeds in the later half of the 19th century was Osborne Reynolds who published a number of papers on the field (Reynolds 1874). Reynolds mistake at the time was to focus on the possibility of entrainment of air within the wake of the propeller blades, a phenomenon currently understood as ventilation. Reynolds does not seem to have at any

point considered the possibility of the vaporization of liquid in propeller wakes. This effect was not truly considered till work conducted by Parsons in 1906 when Froude coined the term cavitation.

A Lifting surface such as a hydrofoil operating in a flow of liquid at sufficiently high speed and angle of attack will be susceptible to the occurrence of cavitation. Cavitation on such a hydrofoil will occur at the point of lowest pressure, which on most hydrofoil designs will occur at the location of the suction peak just behind the leading edge of the foil. Cavitation where it occurs on such lifting surfaces is usually considered detrimental as it results in the loss of performance characteristics and causes flow unsteadiness, leading to the generation of noise and vibration potential causing surface erosion damage to the lifting body. Traditionally the design of hydrofoils has focused on the complete elimination or if not possible then minimization of cavitation effects.

The extent to which cavitation occurs and the size of the cavitating region that develops is dependent on a number of flow conditions and also the geometry of the foil. In order to help clarify the level of cavitation occurring when discussing the phenomenon an ultimately necessary, dimensionless but inadequate parameter of similitude was devised to characterize such flows was determined based on the Euler number. This quantity termed “cavitation number“ K, is defined by the following equation where:

$$K = \frac{P_\infty - P_v}{\frac{1}{2}\rho U_\infty^2}$$

In this equation the static pressure minus the vapor pressure for a given fluid is compared as a ratio to the dynamic pressure. From this equation it is observed that higher cavitation numbers will result in flows with less cavitation i.e. flows with a K value greater than 3 are considered to have almost no cavitation potential and those with very low cavitation numbers in the range of say 0.1 are considered to have a vey high cavitation potential.

According to Franc and Michel (Franc, J., 2006) there are two distinct phases in the development of cavitation experienced by submerged bodies. These two phases are defined as:

- Phase 1: Cavitation inception, this phase describes a period of transition between sub-cavitating flow regimen and a barely cavitating flow regimen.

- Phase 2: Developed cavitation, this phase describes a form of cavitation, which is maintained after nucleation by liquid vaporization effects, and diffusion of non-condensable gasses across a clearly defined two phase interface, in this case a cavity surface.

It is worth noting that a number of texts also include the existence of an additional distinct phase occurring after the development of cavitation defined as super cavitation (Savchenko 2001), where the dimensions of the cavity considerable exceed the dimensions of the submerged body.

Cavitation nucleation as explained above is dependent on the presence of suitable nucleation sites will originate at the location of the minimum value of the systems pressure coefficient C_{Pmin} where:

$$-C_{Pmin} \geq K = \frac{P - P_{\infty}}{\frac{1}{2}\rho U_{\infty}^2}$$

From this the quantity by which the minimum local pressure falls below the vapor pressure can be termed the static delay to cavitation and is a function of the systems nucleation conditions. In most practical engineering situations such a delay is so small that it is standard procedure to take the following as an estimate for the cavitation number at inception where:

$$K_i = -C_{Pmin}$$

Note that the negative sign in the above equation results from the definition of the pressure coefficient where the local pressure is reduced below that of the free stream pressure.

2.1.4 Computational Fluid Dynamics

Whist the Navier-Stokes equations were defined in the early 1800s their complexity hindered their use in the solving of flows over complex geometries. In fact the earliest numerical solution to a complex fluid dynamics problem of flow past a cylinder was not published until 1933 and can be seen at (Thom A. 1933). Additionally one of the earliest computed numerical solutions was produced by (Kawaguti M. 1953) involving two-dimensional flow around a cylinder for a Reynolds number 40 flow using the full Navier-Stokes equations. This process required Kawaguti to work 20 hours a week for 18 months using a desk calculator to solve.

Since this time numerous CFD modelling systems have been developed with the early models generally consisting of in-house codes developed by corporations and were specialised with purposes required by the corporation developing the code. The earliest codes being two-dimensional models using the potential equations with very simple vortex models. As computing power increased common models developed to the point of using Euler equation based systems using turbulent flow models and increasingly complex geometry's. Modern CFD models are capable of using the full Navier stokes equations for highly complex models with complex wake vortex and turbulence models.

Regardless of the modelling system or software package used all approaches follow a similar procedure in the method of producing useable data.

The initial development of a CFD simulation is the pre-processing phase where the system to be analysed is defined. This involves the following steps:

- The geometry or physical boundary of the system to be modelled is defined
- The volume of the system occupied by fluid is divided into discreet volumes or cells, commonly referred to as a mesh.
- The physical modelling is defined, where the chosen equations of motion as well as the physical interactions between fluids and surfaces are defined.

- Boundary conditions of the system are defined where the behaviour and properties of the fluid at the boundaries such as the inlet and outlet as well as on solid surfaces are defined.

With the development of easily accessible and open source CFD software in recent years a number of third party tools have become available for the generation of meshes rather than the use of the CFD software's internal code allowing for much greater manipulation of the mesh creation process. Additionally models are now much easier to imported from a large number of computer aided design (CAD) software's commonly used by manufactures allowing for much more rapid development of CFD models.

Following this pre-processing phase the simulation of the system is started and the equations of the chosen model are solved in an iterative process. Finally after the simulation is completed a post processor is used to analyse and view the results of the simulation and extract any relevant data.

Historically analysis of characteristics and performance of interactions between fluid flows and surfaces has typically required the use of wind tunnel testing to determine approximate values for system parameters and full scale model testing to provide accurate and useable data. With the development of increasingly powerful computers CFD has come to the forefront of tools used in the initial development of designs for numerous manufacturing industries such as aerospace and naval architecture. Until Recently simulations of the more exotic phenomenon such as cavitating flow and other effects were limited to the self-developed "in house" CFD codes. With the introduction of flexible open source software such as OpenFOAM (Open Source Field Operation and Manipulation) the tools to analyse complex flows are now available to academic institutions without the large capital expenditure that might otherwise be required to purchase or develop a software package.

Whilst modern software packages perform with generally acceptable levels of accuracy for most applications this was not so with the earlier versions of CFD software. Due to

these early inaccuracies modern industry has a tendency to mistrust data obtained from CFD techniques discarding it as inaccurate and unreliable, preferring to rely on empirical models developed through mass trials of physical models. This mistrust has resulted in a drive to improve CFD techniques to improve the accuracy of the software with respect to the data gained from empirical methods.

OpenFOAM is a free and open source CFD toolbox and software package produced by OpenCFD Ltd and has a user base of both commercial and academic organisations across a range of both engineering and science based disciplines. This software package is highly developed and includes the capabilities to solve complex flow simulations involving a range of circumstances including chemical reactions, complex turbulence models and heat transfer. This software also includes pre-processing tools such as a meshing tool capable of meshing complex CAD geometry's but does not allow for easy creation of complex geometry's requiring third party CAD software for their generation.

The capabilities of the included solvers in the software range from simple models of incompressible flows to compressible and multi-phase flow simulations as well as buoyancy driven flows among others with a selection of 80 specialised solvers. OpenFOAM also provides a selection of turbulence models including the Reynolds averaged Navier-Stokes (RANS) and large eddy simulation (LES) methods. Additionally the incorporated SnappyHexMesh mesh generation tool provides the ability to generate highly detailed and customisable meshes around complex geometry's, however the software is also capable of accepting meshes generated from a range of third party meshing tools such as Netgen, Gmesh and Blender.

When simulating fluid flows OpenFOAM has a suite of numerical tools used to solve a range of problems. This includes methods of solving problems where matter is represented both as a continuum and as discreet particles. When solving equations based on a fluid continuum OpenFOAM uses a finite volume method (FVM) where matrix equations are constructed using the FVM applied to arbitrary shaped cells. Additionally a segregated, iterative solution is used where the governing equations of the system are

reduced to separate matrix equations created for each individual equation and are solved within an iterative sequence. Also equation coupling is used where coupling between related properties such as pressure and velocity are performed using adapted versions of well-known algorithms such as PISO.

2.1.5 Turbulence Modelling

Turbulence is a key issue in most engineering applications of CFD techniques. This is a result of nearly all engineering problems having some form of inherent turbulence and thus requiring a method of turbulence modeling.

Turbulence is best defined as a state of motion of a fluid best defined as by what appears to be random and chaotic vorticity. In situations where turbulence is present it has a tendency to dominate all other flow characteristics, usually resulting in increased energy dissipation, fluid mixing, heat transfer and drag effects on submerged bodies. Modeling of real turbulence requires that it be done in three dimensions; this is a result of the requirement of the ability of turbulence to create new vorticity from existing turbulence. This is something that can only occur when the necessary stretching and turning in three dimensions can be modeled.

For modeling turbulence there are a number of systems available with the most common methods including models based on the Large Eddy Simulation (LES) scheme, the Reynolds Averaged Navier-Stokes (RANS) Model and Direct Numerical Simulation (DNS) scheme.

Of the above three methods DNS is considered to be the most accurate modeling method for CFD simulations, this is as a result of this methods solving of each point along the surface of a flow field. The disadvantage of such a method is that it requires excessive processing power and extended periods of time to both implement and run. For tis reason such a method is seldom used except in the case of where extreme accuracy is required and both time and a suitable computing resource are available.

The principle behind the operation of LES simulation is the utilization of low pass filtering. This technique is applied to the Navier-Stokes equations to eliminate turbulence effects on smaller scales within the system. The consequence of this filtering technique is a reduction on the processing power required to complete the simulation.

The effect of using LES simulation is the resolving of large scales of floe field solutions with better fidelity that that offered by RANS techniques in addition it also models the smallest and most computationally dependent scales rather than resolving them using the extremely costly DNS method. This method allows for turbulent flow fields around complex geometry's being resolved with reasonable accuracies using supercomputing resources.

The RANS method for turbulence modeling is one of the more common methods for simulating turbulence in fluid flows. Whilst there are a large number of varied RANS models the basic operating principle is shared among all, this principle being the objective of computing the Reynolds stresses using one of three methods. These three methods are the liner eddy viscosity mode, non-linear eddy viscosity model and the Reynolds stress model.

In this project a RANS two-equation model is used where turbulence needs to be considered. The selected model is the RANS k-ω SST, which includes two extra transport equations to represent the turbulence of the fluid. The first included transport variable is the turbulent kinetic energy k, and the second is the specific dissipation ω. In this system k determines the energy in the turbulence whilst ω determines the scale of the turbulence. This two-equation model allows for the accounting of historical effects such as convection and the diffusion of turbulent energy. The reason for the selection of this model for simulations is that it provides a good all-round turbulence model without requiring an excess of additional processing power. This is a result of the model combining the best aspects of both eddy and viscosity modeling techniques. The use of the k omega formulation in the inner sections of the boundary layer makes said model directly usable all the way through to the vicious sub layer. The SST component also allows for switching to a k-epsilon behavior in the free stream avoiding a common k-omega problem where the model tends to be too sensitive or free stream turbulence properties. However it should be noted that the accuracy of RANS turbulence modeling is considered to be somewhat dubious exemplified by (Spalart 2000) where it is stated

that RANS models of any complexity have “no reasonable claim” to provide accurate stresses in complex flows.

Accurate representation of the total kinetic energy k, as a boundary condition when using CFD techniques is important if the flow is to be accurately predicted. This is even more so in the simulation of high Reynolds number flows where such turbulence may have greater effect. The value for TKE may be calculated using the following equation where:

$$k = \frac{3}{2}(UI)^2$$

Where I is the Initial turbulence intensity as a percent and can be defined by:

$$I = 0.16\, Re^{-1/8}$$

The specific turbulence dissipation rate ω, is defined as the rate at which TKE is converted into thermal internal energy per unit volume and time where;

$$\omega = \frac{\epsilon}{k\beta}$$

Where β is a model constant (β = 0.09) and ε is the turbulence dissipation described by:

$$\epsilon = \beta\, \frac{k^{\frac{3}{2}}}{l}$$

Where l is the turbulence length scale is not a well-defined quantity and for most situations is best set at approximately 5% of the channel height or hydraulic diameter etc. This has the effect of ensuring that the turbulence length scale does not exceed the size of the problem resulting in turbulent eddies far larger than would ever be expected.

2.1.6 Literature Review

Empirical data is available for a range of hydrofoil designs derived through experimental methods. Force coefficients such as lift and drag ratios have been obtained for a large number of shapes including simple geometric designs such as wedges, circular cross sections and flat plates as well as more geometrically complex shapes such as air and hydrofoils. Symmetrical hydrofoil shapes such as those described by (Keerman R. 1956) serve important functions on many watercraft as both lifting surfaces as well as support struts and non load bearing fairings an a range of structures. These designs meet the general requirements for such an application; as they are easy to design with a low drag, low critical cavitation number and high strength.

These characteristics of symmetrical cross section hydrofoils are agreed with in the wartime report (Land, Norman S. 1943) where his investigation shoved that such a hydrofoil (in this case a NACA 66 s-209) is capable of producing a high lift to drag ratio at speeds that would be considered reasonable for modern watercraft and displayed a low critical cavitation number, able to resist serious cavitation effects at to an angle of 12 degrees at a speed of 40 meters per second.

Cavitation is one of the most important effects suffered by hydrofoils. This phenomenon occurs when the local pressure drops below the fluids vapour pressure causing a change in phase. This effect can cause considerable damage to solid surfaces and can also have dramatic effects on the performance of submerged bodies. For this reason the effects of cavitation on hydrofoils have been an area of interest for CFD researchers. Research conducted by (Shen Huang et al. 2010) into the modelling of a NACA 66 type hydrofoil using Fluent CFD software to model steady cavitating flow at a range of angle of attacks and cavitation numbers shows that CFD software is capable of providing a good estimation of the effect on a hydrofoil at such conditions. Although their results did show that at sections where the flow separated from the foil that the CFD software did show variance to the experimental results outside what could be considered normal experimental variation.

Investigation using numerical methods on 2D hydrofoils on cavitating flows was also carried out by (Greeshma P. R. et al. 2012). This simulation was carried out on a non standard symmetrical hydrofoil at an angle o attack of seven degrees at cavitation numbers ranging from 2.5 to 4. This research showed that for this particular foil and orientation incipient cavitation deployed at an approximate cavitation number of 3 to 3.5 and evolves to full unsteady cavitation around a cavitation number of 4, with super cavitation conditions being met on further increase of the cavitation number. Also from this model it was determined that as the cavitation effects occur that lift decreases and drag increases.

Unsteady turbulent cavitation effects on a NACA-0015 section hydrofoil was studied by (Kim, Sung-Eun. 2009) using the OpenFOAM toolkit. This simulation used a multi phase solver with a liquid vapor mix modeled as an interpenetrating continuum with hybrid RANS/LES turbulence model. The results gained from this simulation for the lift and drag coefficients in a range of cavitation numbers were found to be in good agreement with the experimental data for this hydrofoil in respect to mean values, root mean squared values and spectral contents.

Simulation of cavitating flows on a symmetrical section hydrofoil using OpenFOAM's interPhaseChangeFoam was carried out in (Gosset 2010). Results from this research showed that attempting to model cavitation effects on a foil using cavitatingFoam produced highly unreliable results that did nor reflect real world cavity dynamics where using interPhaseChangeFoam still produced unreliable results (better than cavitatingFoam) but tended to better reflect real world cavitation dynamics. The conclusions drawn by Gosset is attempting to model such a situation as this for extracting hydrofoil performance characteristics using OpenFOAM is that results within an order of magnitude to experimental results are of an acceptable nature.

3.0 Construction of SimpleFoam Sub-Cavitating Simulations

3.1 Constructing NACA66-012 Hydrofoil Model and Flow Domain Meshing

As stated above a NACA66-012 hydrofoil model was selected for testing as data was found to be available for this hydrofoil in a wide range of flow conditions. As with most standardized hydrofoil design geometry data for the foil is defined as stations and ordinates as percent of the chord. In this case station refers to the percentage of chord from the leading edge of the foil and ordinate the normal distance from the chord line to the surface of the foil.

Table 1: Design Geometry of NACA66-012 Hydrofoil

NACA Profile 66-012		
(Stations and ordinates given as per cent of airfoil chord)		
x	y	dy/dx
0.0000	0.0000	N/A
0.5000	0.9038	0.8364
0.7500	1.0859	0.6399
1.2500	1.3525	0.4534
2.5000	1.8067	0.3142
5.0000	2.4936	0.2428
7.5000	3.0378	0.1968
10.0000	3.4933	0.1696
15.0000	4.2340	0.1292
20.0000	4.7996	0.0991
25.0000	5.2364	0.0763
30.0000	5.5656	0.0560
35.0000	5.7987	0.0376
40.0000	5.9424	0.0197
45.0000	5.9981	0.0022
50.0000	5.9642	-0.0163
55.0000	5.8339	-0.0366
60.0000	5.5857	-0.0659
65.0000	5.1477	-0.1097
70.0000	4.5122	-0.1398
75.0000	3.7677	-0.1571
80.0000	2.9432	-0.1706
85.0000	2.0807	-0.1723
90.0000	1.2346	-0.1643
95.0000	0.4738	-0.1352
100.0000	0.0000	-0.0016
L.E. radius = 0.870 percent chord		

Using the data from the table above a model of the hydrofoil was constructed using Dassault Systems Solidworks. Using the dimensions provided by Keerman the model was constructed with a chord length of 3.3" and a span of 2.9" (0.084 meter chord and 0.734 meter span). Choosing to exactly replicate the dimensions of the foil was the result of previous scale testing's using a one meter by one meter scale model did not produce desirable results.

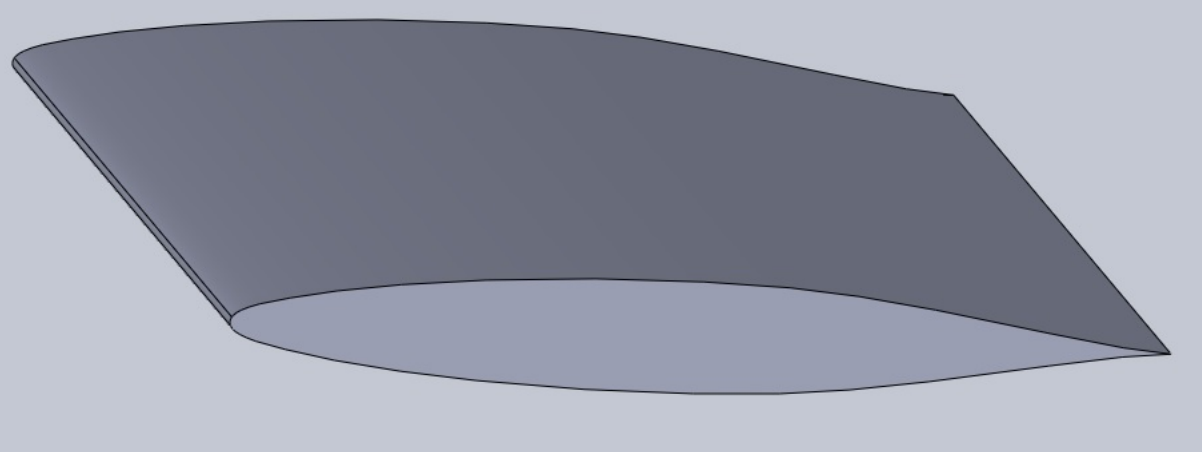

Figure 4: Image of Hydrofoil Design From Dassault Systems Solidworks

This hydrofoil model was then converted to a STereoLithography or Standard Tessellation Language (.STL) format. When creating this model the solid body is divided into triangular segments. A high refinement level was used in this creation with surfaces having a maximum 0.5-degree angle of incidence and a maximum deviation from the solid surface of $6x10^{-4}$ cm. This file format was chosen, as it is a common file format that is accepted by most common third party meshing tools as well as OpenFOAM's inbuilt meshing tool. This STL file format defines complex geometries through a raw unstructured triangulated surface by the unit normal and vertices of the triangles using a three dimensional Cartesian coordinate system.

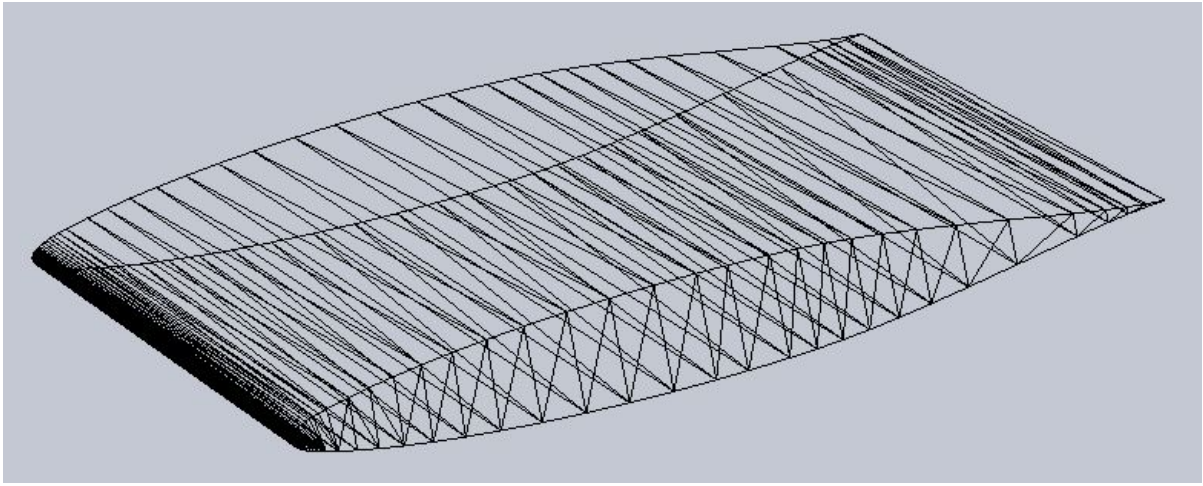

Figure 5: Image of STL of NACA 66-012 Hydrofoil

The created STL file of the Hydrofoil consists of 1796 individual triangular sections. Whilst theoretically able to handle both ASCII and binary formats when using this file with both Netgen and snappyHexMesh the binary format appears to fail to mesh with a consistent level of accuracy thus ASCII is the preferred format for this file.

When constructing the flow domain it was important to select a domain size great enough to model all the effects occurring both in front of the hydrofoil and behind but not so great as to increase the amount of computational power required extending the required time to run the simulation. In order to best accommodate these requirements a domain of 10 chord lengths long (parallel to flow vector) and 3.25 chord lengths high (normal to flow vector) and 1 foil span wide was chosen with the center of rotation of the hydrofoil placed 3 chord lengths from the inlet boundary and centered on the vertical axis.

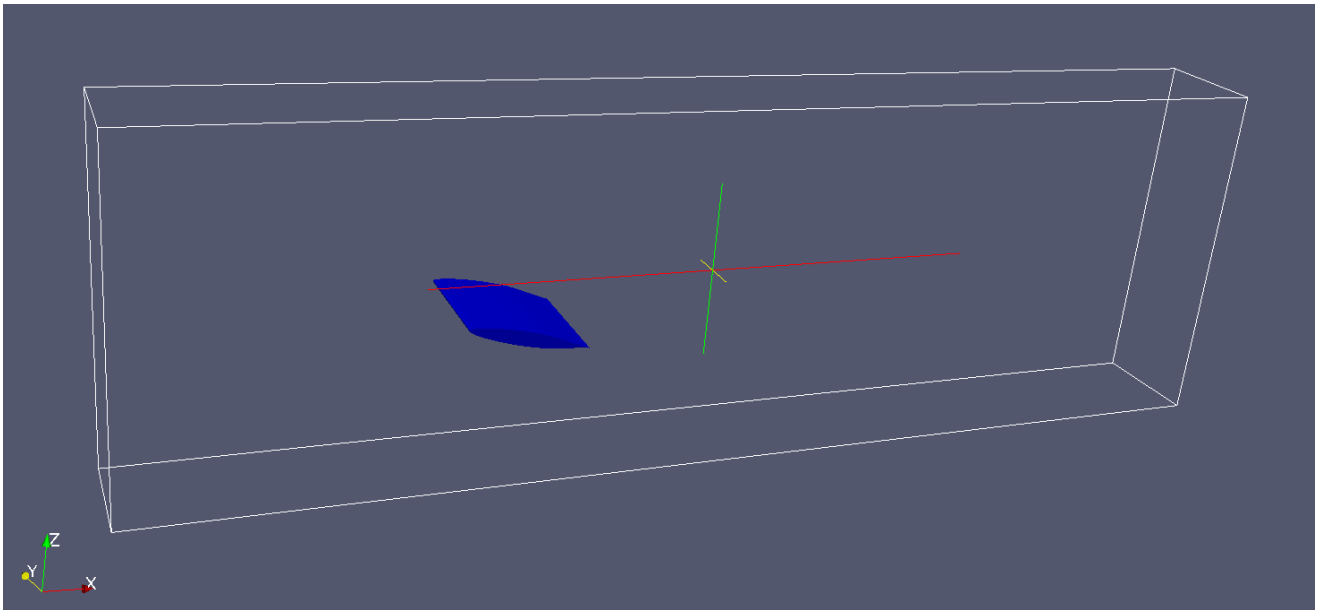

Figure 6: Diagram of NACA66-012 Foil in Flow Domain

Using the inbuilt snappyHexMesh function within OpenFOAM the foil was meshed into the flow domain at the beginning of each simulation. Using a level (5,6) refinement with 3 additional boundary layers and a refinement box surrounding the foil a mesh was created that has a relatively coarse structure at distance from the hydrofoil and increasing density as the distance to the foil decreases. This allows for an approximate model of fluid as it moves away from the foil whilst attempting to model accurately flow close to the foil. This resulted in a mesh of approximately 5.6 million cells varying slightly when changing the angle of attack of the foil and re-meshing.

Prior to the selection of snappyHexMesh as the meshing tool to be used, other meshing tools such as Gmesh and Netgen were trialed but failed to provide adequate and repeatable results when importing into OpenFOAM. Thus due to the instability and variance in meshes that were created these meshing tools were discarded as potential options and it was decided to use the inbuilt tools.

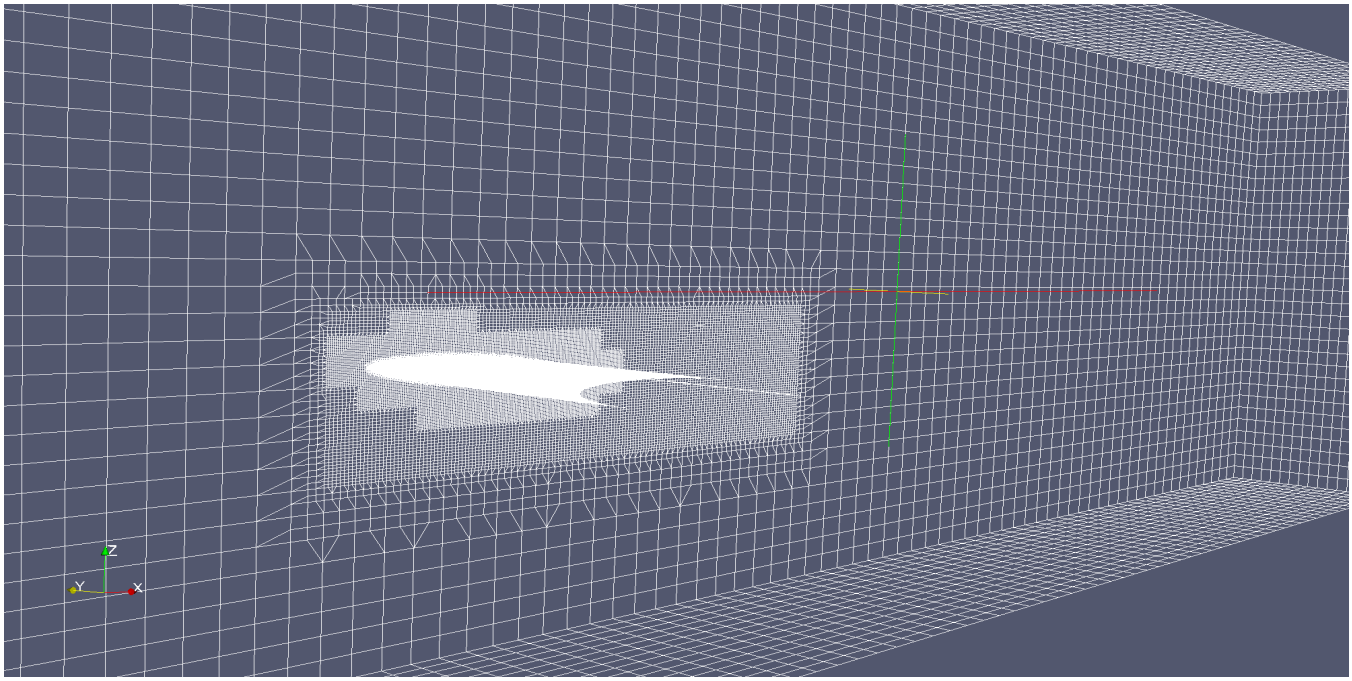

Figure 7: Wire-Frame Diagram of Mesh Surrounding NACA66-012 foil at 5° Angle of Attack

3.2 Determining Field Constants and transport Properties

Before running each simulation there are a number of transport properties and variables that need to be calculated and input into the appropriate files in the OpenFOAM case directory. These variables include the kinematic viscosity of the fluid, the turbulence kinetic energy and the specific diffusion rate.

As the Reynolds number is provided for each flow velocity and angle of attack the kinematic viscosity needs to be adjusted slightly for each simulation where:

$$Re = \frac{V.c}{\nu}$$

Whilst this generally resulted in a change of less than a couple of percent from the standardized value of $1 \times 10^{-6}\ m^2/s$ used for water at approximately room temperature it did eliminate this as a possible source of deviation between theoretical and experimental results.

Additionally the turbulence kinetic energy k, and specific dissipation rate ω, needed to be calculated for each flow velocity used, as both are a velocity dependent term. Values for each are displayed in the following charts. Where they are calculated using:

$$k = \frac{3}{2}(UI)^2$$

and

$$\omega = \frac{\epsilon}{k\beta}$$

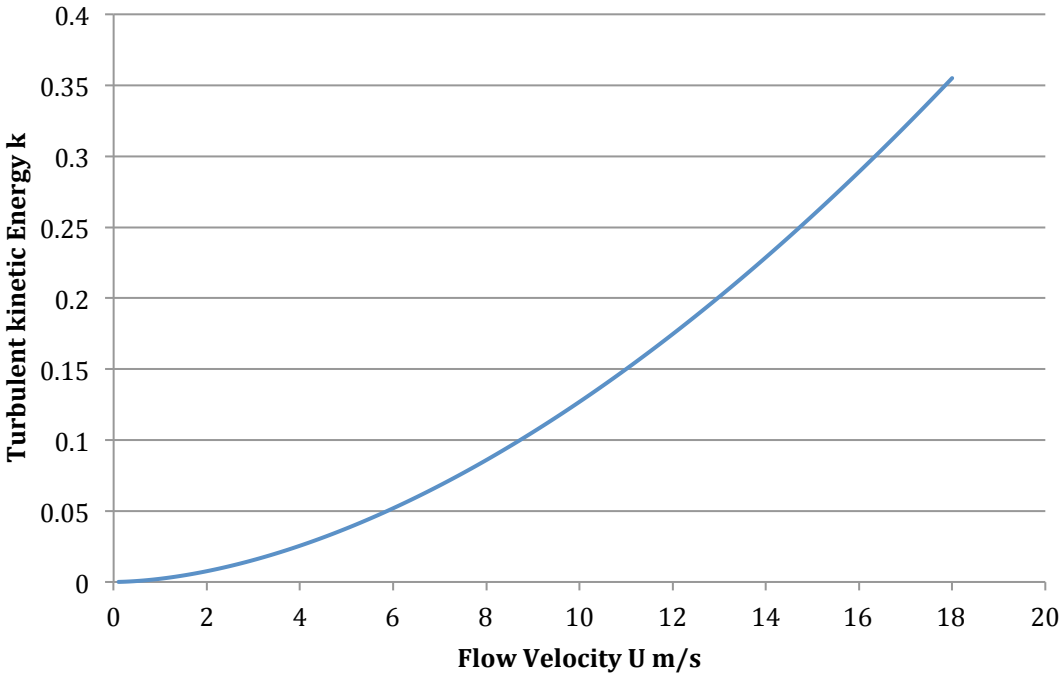

Figure 8: Turbulent Kinetic Energy for Given Flow Velocities

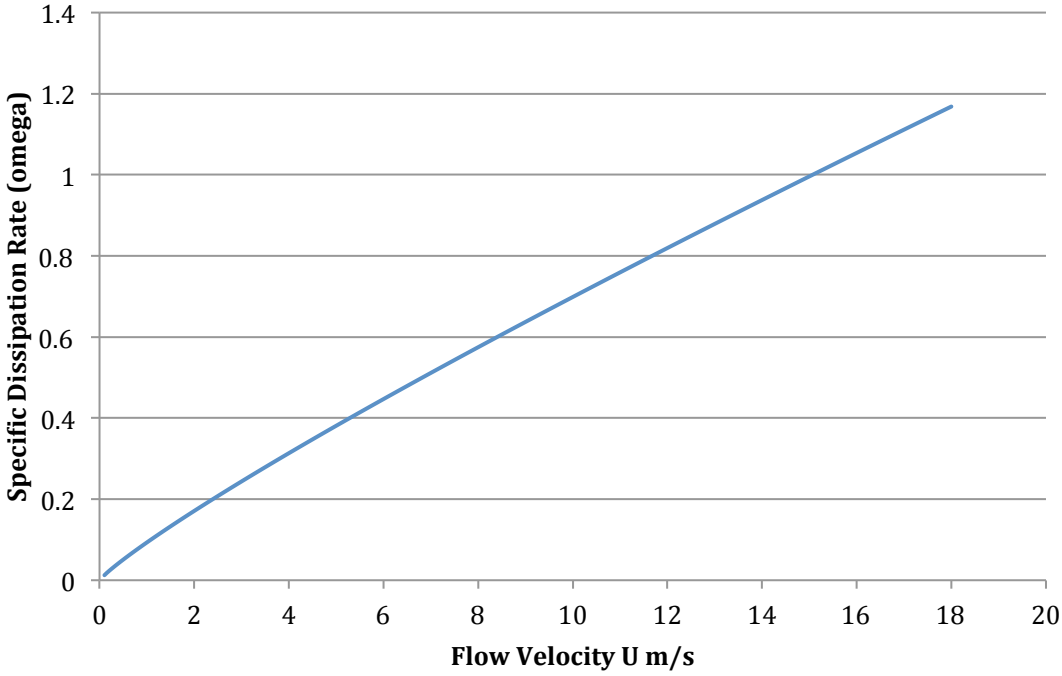

Figure 9: Specific Dissipation Rate for Given Flow Velocities

3.3 Simulation of Foil Performance in Sub-Cavitating Flows

Following the construction of the case files each simulation was run for the given angles of attack and speed. The simulations were run for 800 seconds in half-second time steps and the results recorded for intervals of every 12.5 seconds. Such a long time period for the simulation was set as to ensure that for those flows at higher speeds and angles of attack would have greater time to reach convergence and those that only reach a quasi static state would produce enough data to calculate average performance characteristics. However during to the relatively large number of cell used in the simulation a number of preprocessing steps needed to be completed prior to running. Firstly using the parDecompose function the domain was divided into a number of sections and each section assigned to a computer processor for operation and on the completion of the simulation the subdivisions were recombined into a single field. Additionally to reduce the time required to convergence the potentialFoam function was run to initialize a potential field across the domain and reduce overall running time by ensuring the flow was partially resolved before the simulation started.

During the simulation a number of post processors were set to produce data. Among these processors were two scripts designed to produce a log of the forces acting on the hydrofoil in each Cartesian axis and a second script designed to calculate coefficients of lift and drag from these forces as well as calculate the pitching moment of the hydrofoil.

3.4 Ensuring Data Extracted from Simulations is Valid for Use

For stead state and quasi-steady state solutions there are three conditions that need to be met in order for there to be reasonable confidence in the data that is produced. When looking for convergence in solutions the most common mistake made is to only consider the values of the residuals, however in reality to be truly sure of convergence values of points of interest should also be monitored and it should be ensured that the domain has an imbalance of less than 1%.

Residuals of the flow are defined, as the difference between the actual values and the values produced by the software package, thus are essentially the recording error for the data. For each simulation the residual values for each velocity axis as well as pressure, turbulent kinetic energy and specific dissipation rate were monitored. It was intended for the simulation to be valid that the residuals meet a point where there is no oscillation or variance or that the RMS value of each residual should not exceed a value of between 10^{-4} and 10^{-5}.

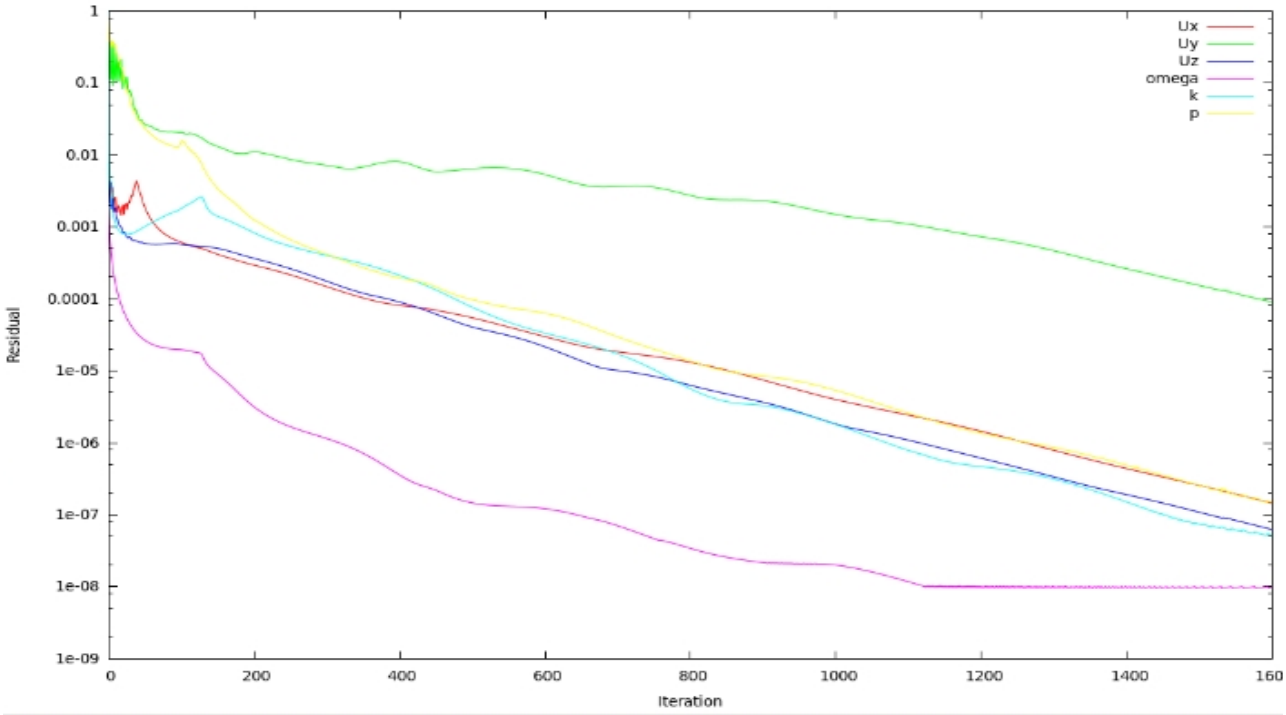

Figure 10: Residual Plot for U = 9.45 m/s and α = 2°

Note looking at this plot of residuals above it is apparent strictly from this data that the residuals would have been in a valid range by around the 800 time step mark however running for the additional 800 time steps has produced slightly better results. Additionally it is valid to run the simulations for such a long period as higher angles of attack and velocities will take longer to meet convergence. Additionally in this plot the residuals for the velocity in the y-axis appear to be several orders of magnitude greater than all other values. This is an inherent property of the design of the simulation where there is near no flow in the y direction resulting in there being large cumulative recording errors for such data.

As stated above monitoring points of interest to observe the occurrence of having reached a steady state solution is an important part of verifying convergence. For the simulations both the coefficients of lift and drag were closely monitored throughout the simulation.

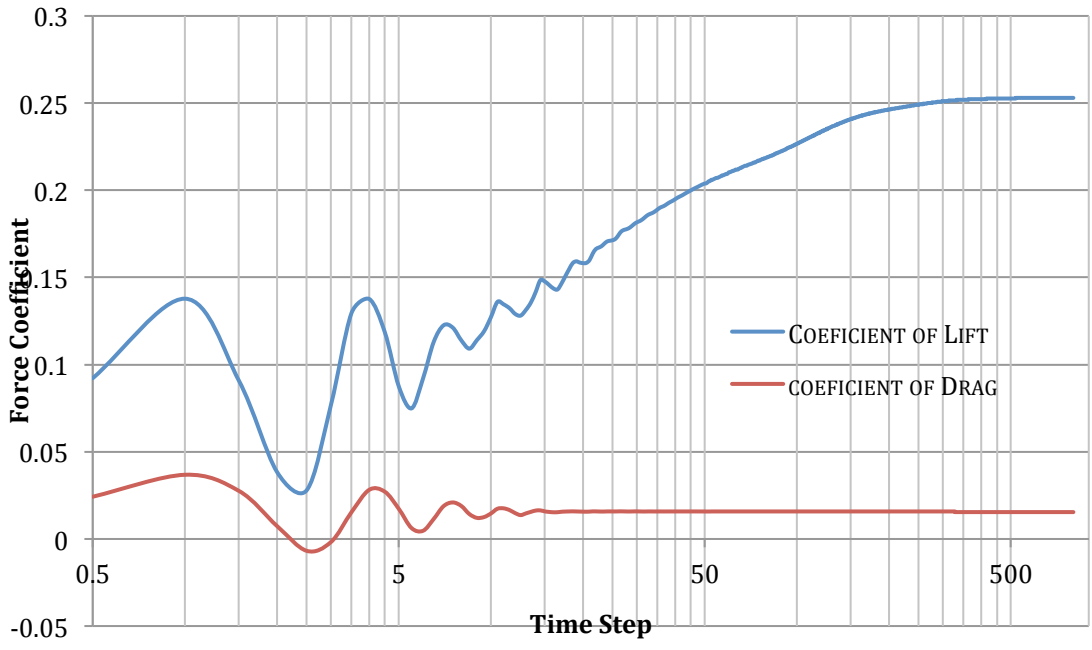

Figure 11: Force coefficients for U = 9.45 m/s and α = 2°

Note in this chart that the x-axis scale is logarithmic to emphasize the oscillations towards the beginning of the simulation. Also worth noting that whist the coefficient of drag reaches steady state within 20 time steps, whilst it is nearly 500 time steps before the coefficient of lift reaches a stead situation.

Finally domain balancing was not considered as a tool for verifying convergence in these simulations as it was unable to be determined if a tool for assessing this parameter was available in the OpenFoam software package.

3.5.1 Sub-Cavitating Results for Flow Velocity's of 9.45 Meters per Second

The first series of simulations were run at a flow velocity of 9.45 m/s at positive angles of attack ranging from 0° through to 13° at 1° increments. These simulations were run using OpenFOAM's simpleFoam solver model. This solver utilizes an incompressible stead state model with included turbulence modeling. Following this the foil was tested at random negative angles of attack in the same manner as the experimental data to prove the foils symmetrical nature. From these simulations coefficients for lift as well as drag and quarter chord pitching moments were extracted. To obtain these performance criteria pressure was integrated along the surface of the hydrofoil and the resulting vector split into components and substituted into the equations defined in the background theory. These results were then compared to experimental results from (Keerman 1956).

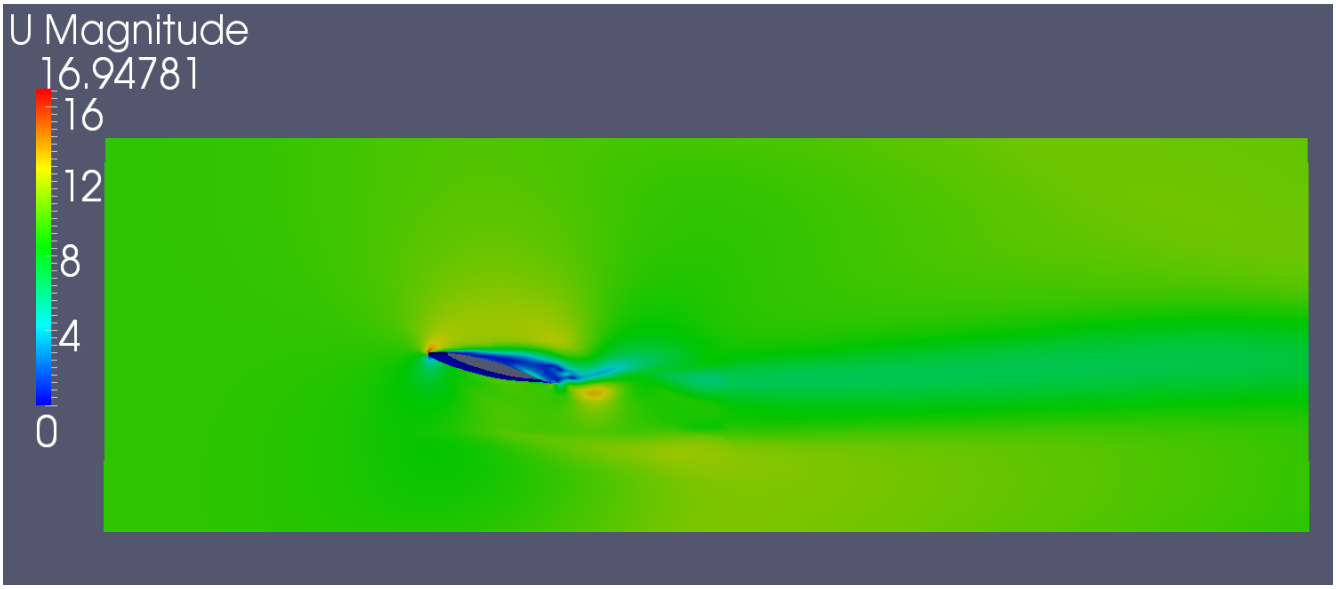

Figure 12: Velocity Field of NACA66-012 Foil at U =9.45 m/s and α = 13°

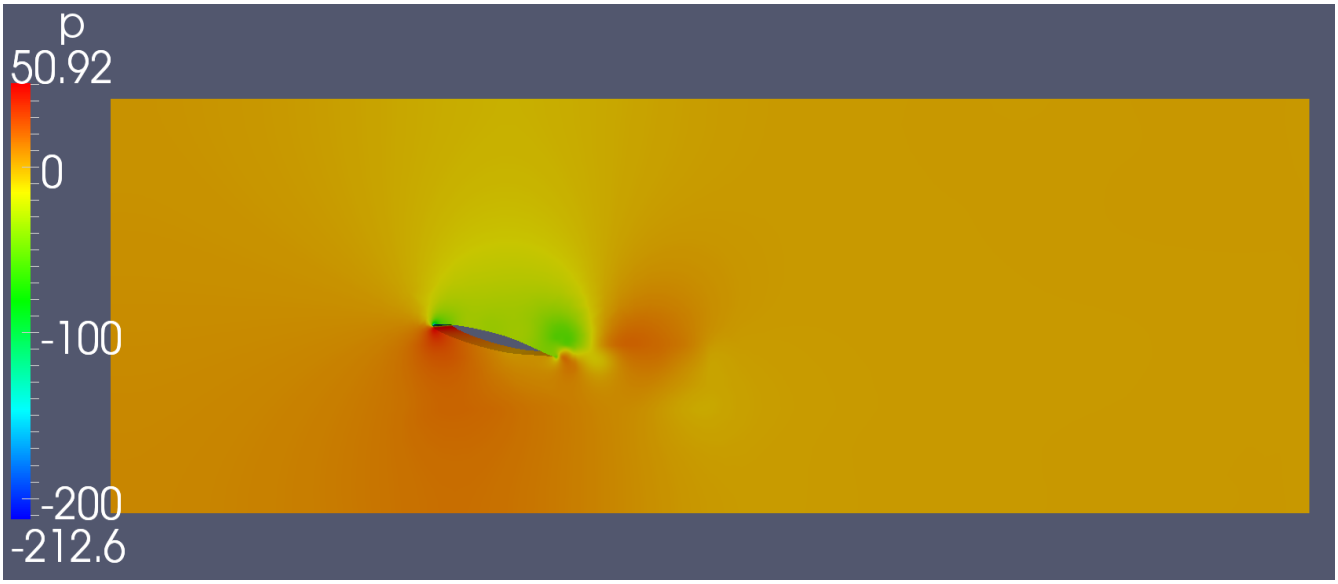

Figure 13: Pressure Field of NACA66-012 Foil at U =9.45 m/s and α = 13°

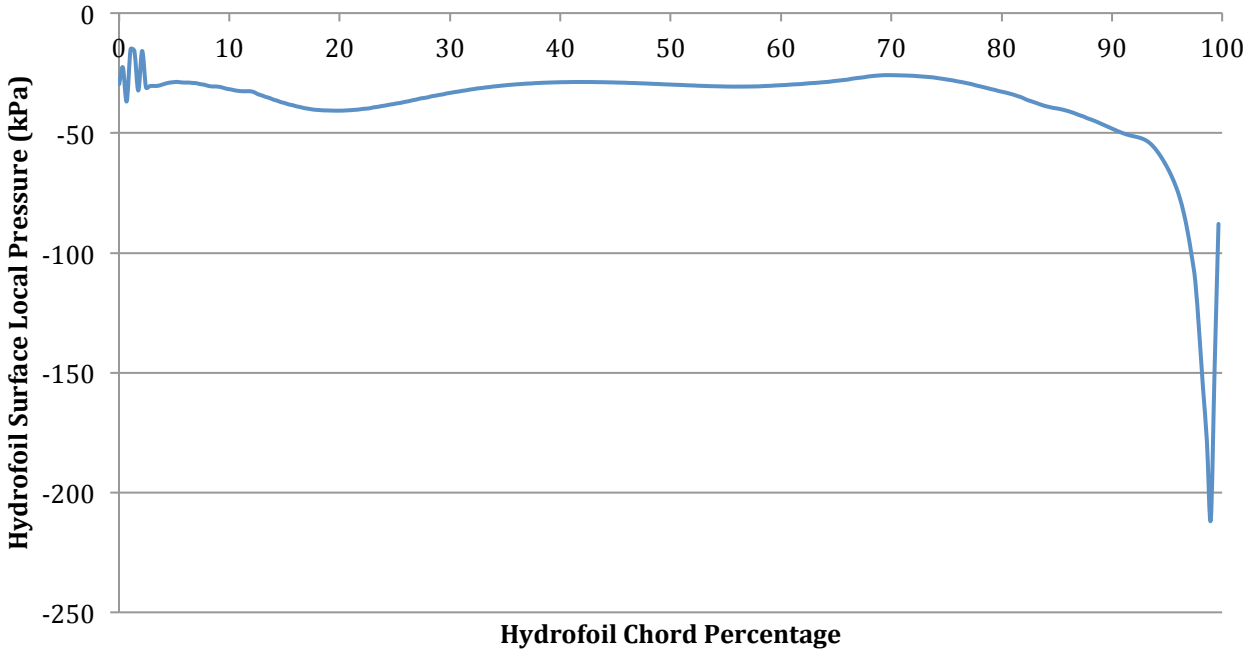

Figure 14: Pressure Across Top Side of NACA66-012 Foil at U =9.45 m/s and α = 13°

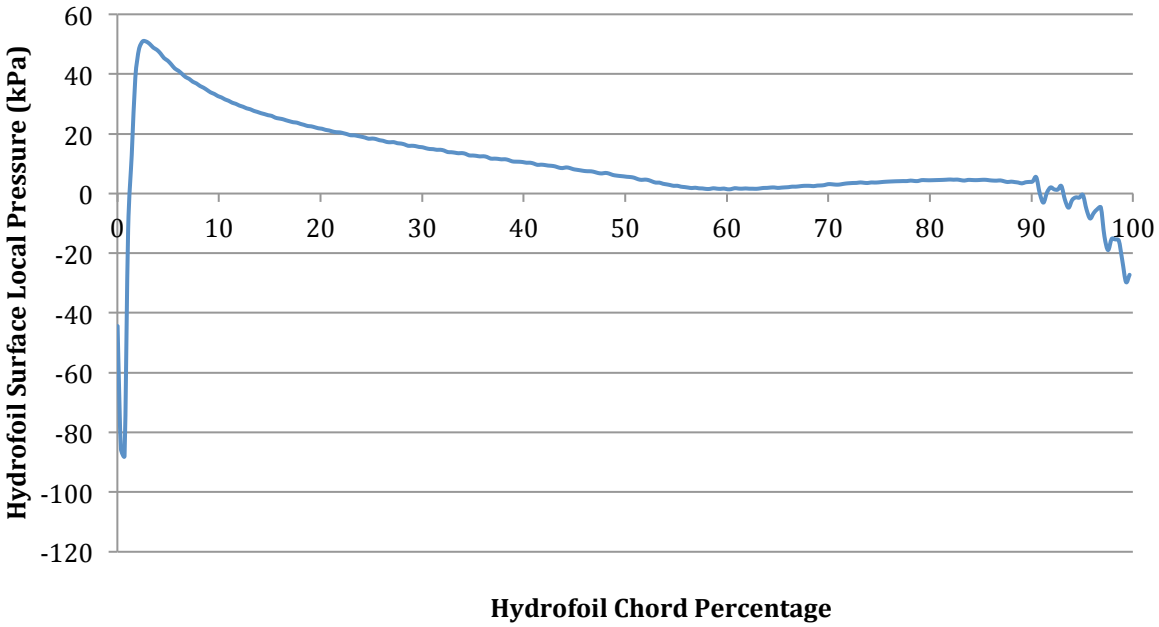

Figure 15: Pressure Across Under Side of NACA66-012 Foil at U =9.45 m/s and α = 13°

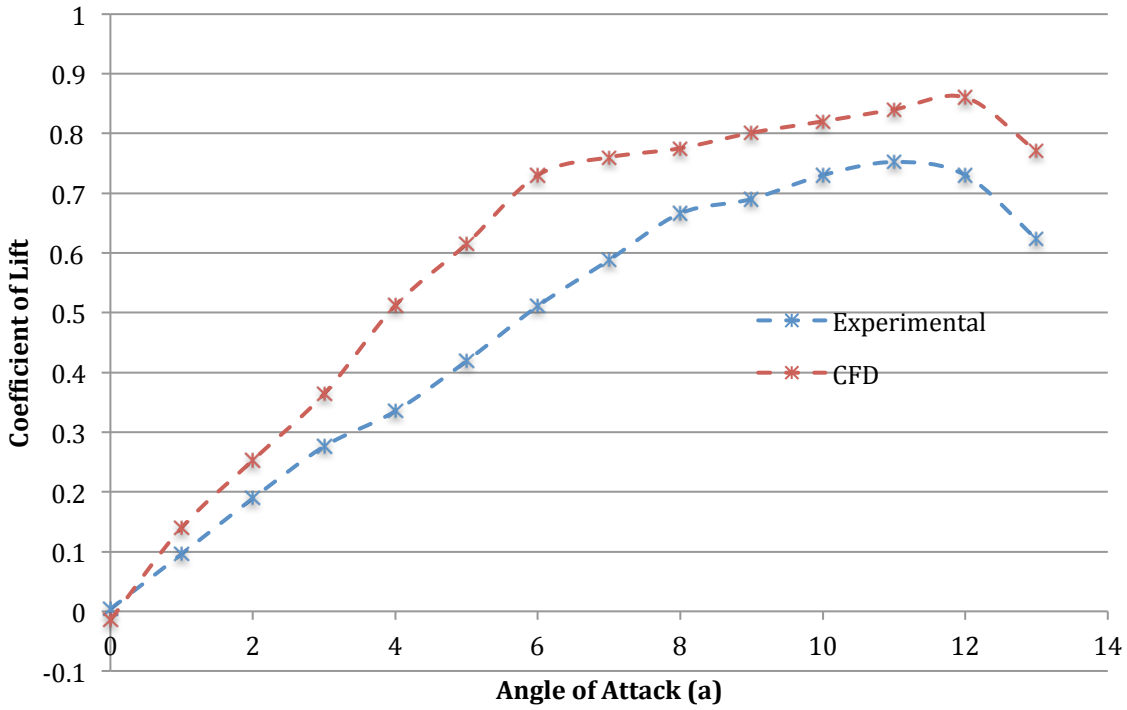

Figure 16: Comparison of Coefficients of Lift at U = 9.45 m/s

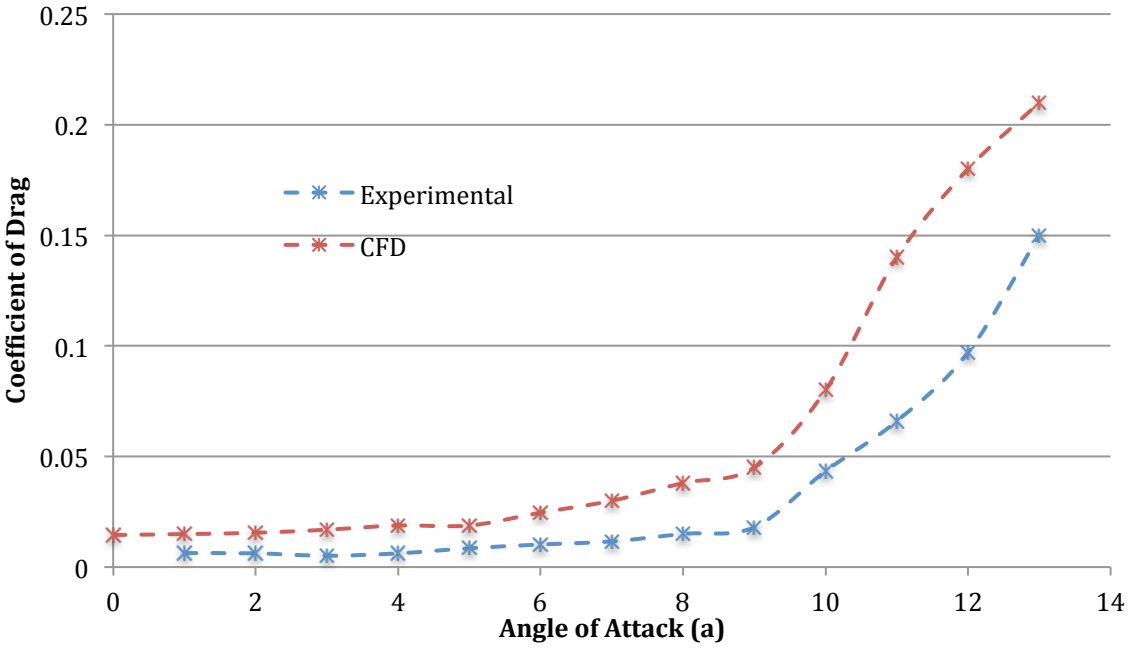

Figure 17: Comparison of Coefficients of Drag at U = 9.45 m/s

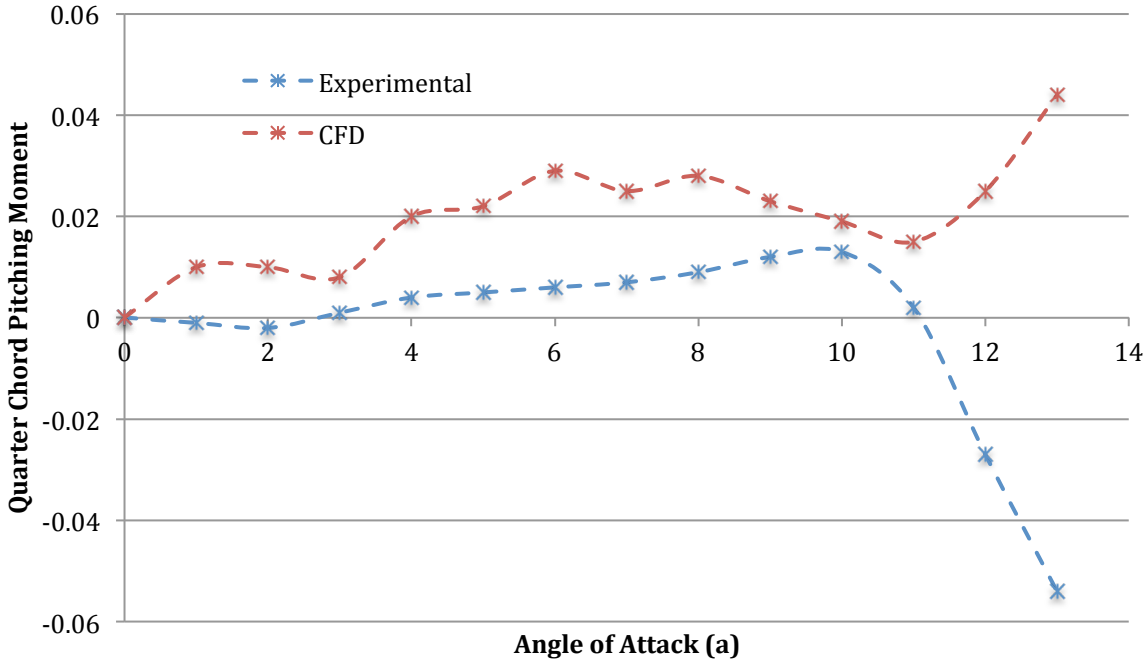

Figure 18: Comparison of Quarter Chord Pitching Moments at U = 9.45 m/s

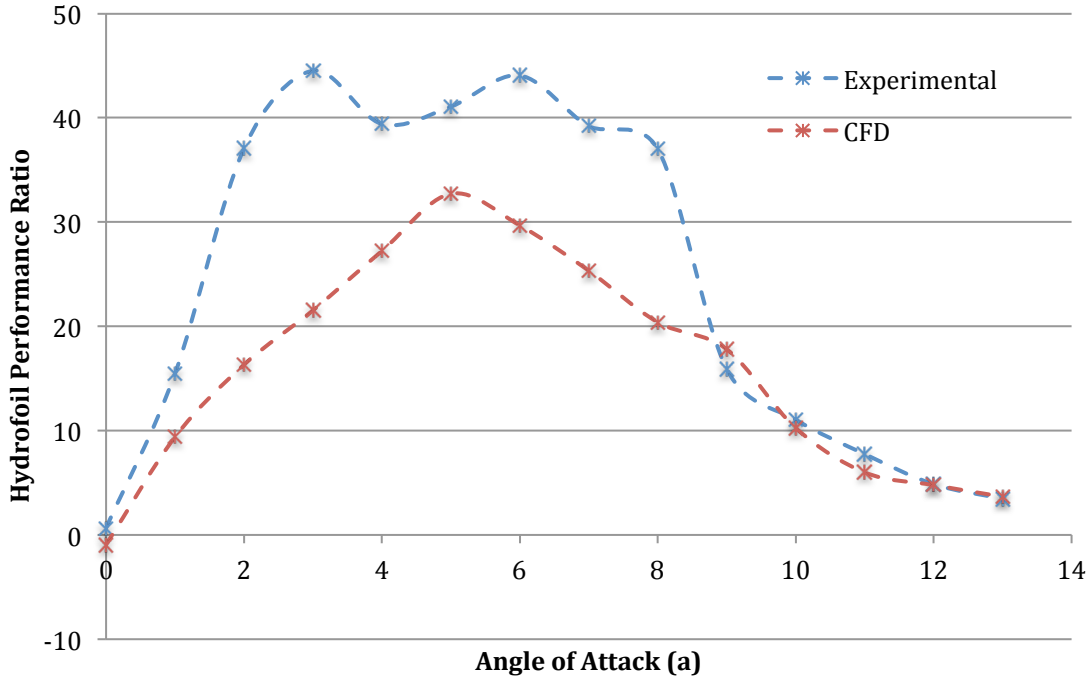

Figure 19: Performance Ratio of NACA66-012 Foil at U =9.45 m/s

3.5.2 Sub-Cavitating Results for Flow Velocity's of 12.55 Meters per Second

The second series of simulations were run at an increased flow velocity of 12.55 m/s at positive angles of attack ranging from 0° through to 11° at 1° increments. The reason for the decrease in total range of angle of attack is that for this flow velocity an increase in angle of attack above 11 degrees will result in incipient cavitation conditions. Following this the foil was again tested at random negative angles of attack in the same manner as the experimental data to prove the foils symmetrical nature. From these simulations as before coefficients for lift as well as drag and quarter chord pitching moments were extracted. Using the same process to obtain these performance criteria, pressure was integrated along the surface of the hydrofoil and the resulting vector split into components and substituted into the equations defined in the background theory. These results were then compared to experimental results from (Keerman 1956).

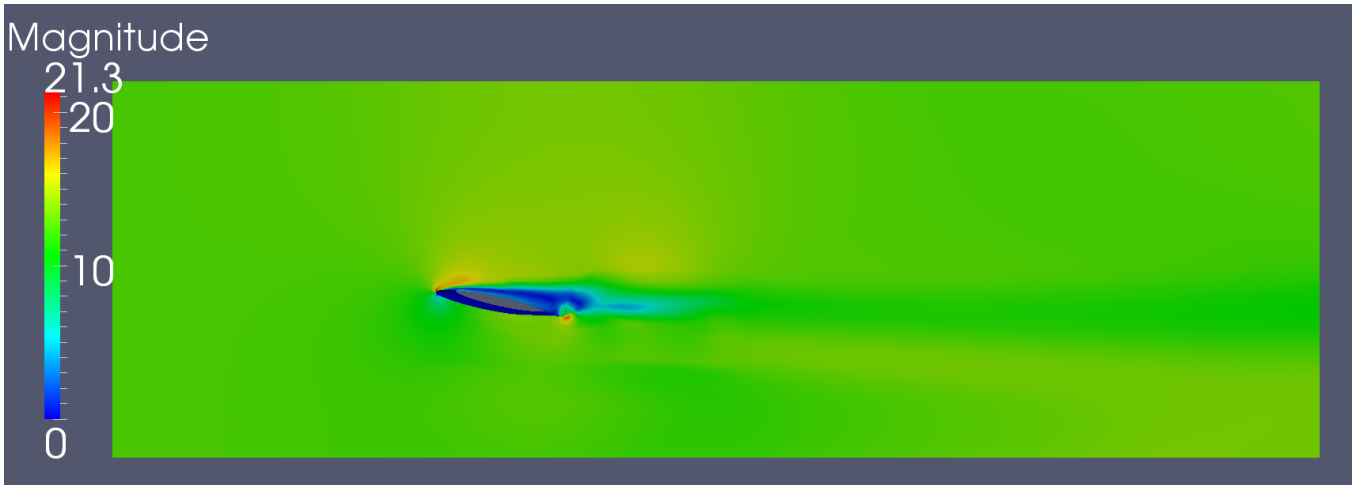

Figure 20: Velocity Field of NACA66-012 Foil at U =12.55 m/s and α = 11°

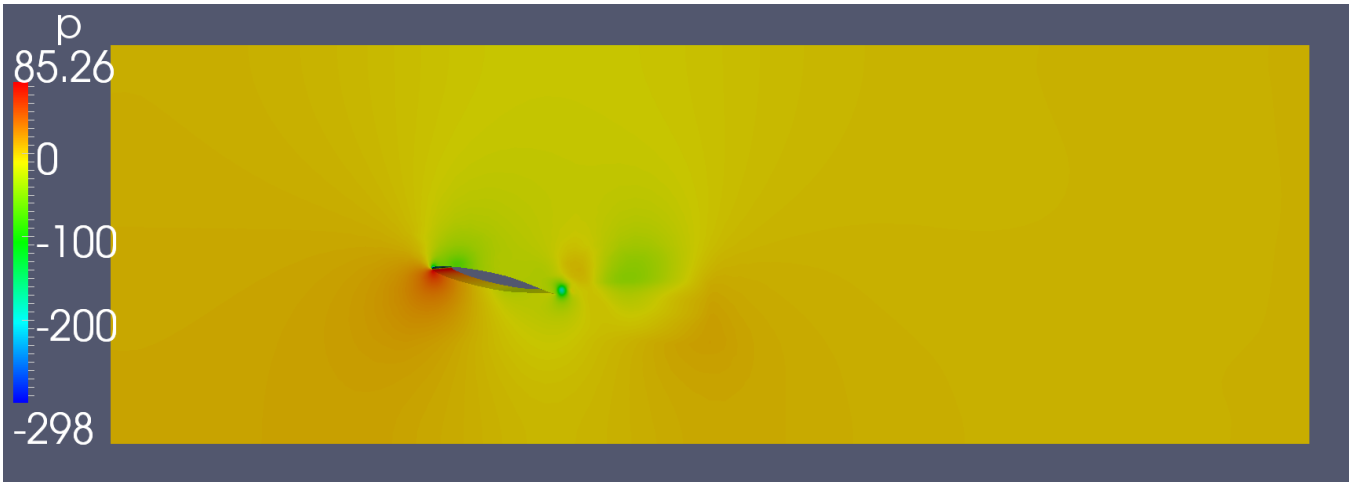

Figure 21: Pressure Field of NACA66-012 Foil at U =12.55 m/s and α = 11°

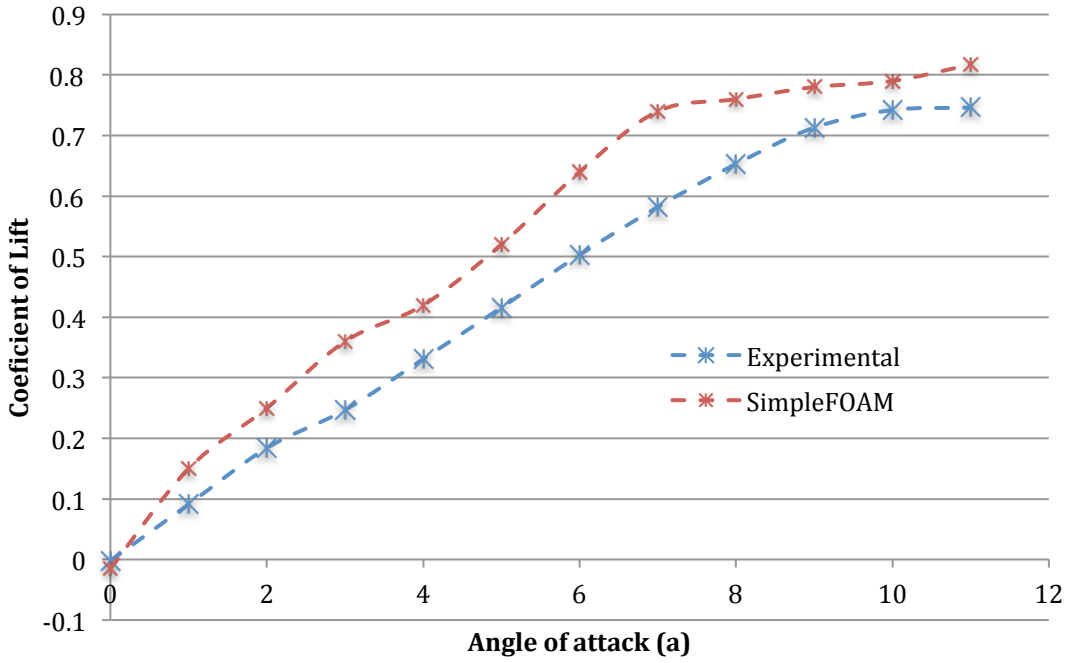

Figure 22: Comparison of Coefficients of Lift at U = 12.55 m/s

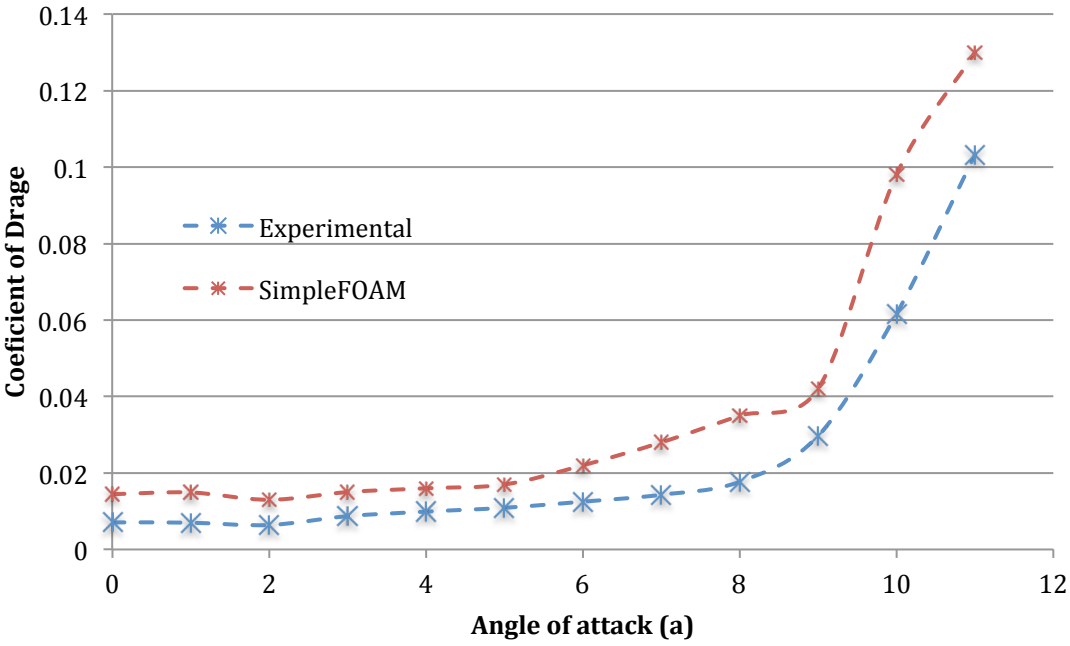

Figure 23: Comparison of Coefficients of Drag at U = 12.55 m/s

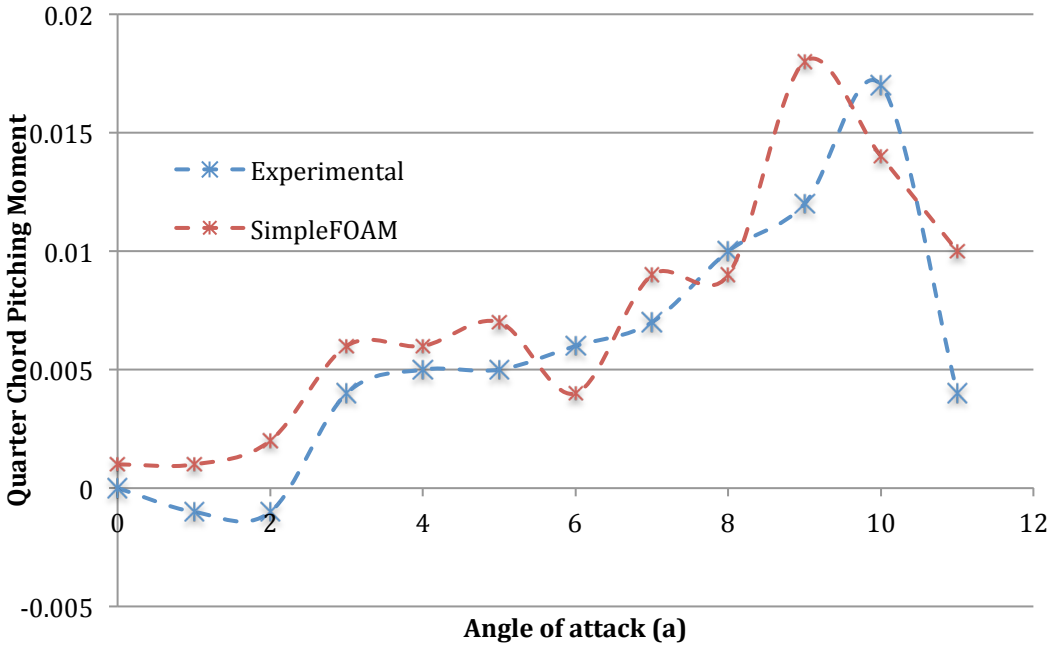

Figure 24: Comparison of Quarter Chord Pitching Moments at U = 12.55 m/s

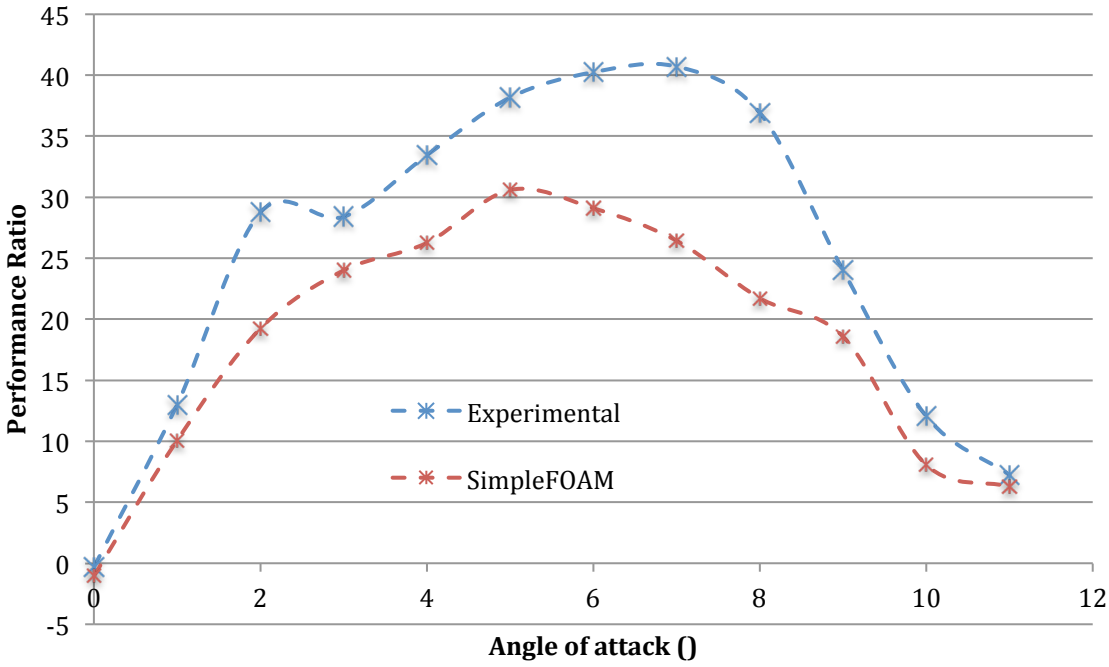

Figure 25: Performance Ratio of NACA66-012 Foil at U =12.55 m/s

3.5.3 Sub-Cavitating Results for Flow Velocity's of 17.50 Meters per Second

The final series of sub-cavitating simulations were run at a further increased flow velocity of 17.50 m/s at positive angles of attack ranging from 0° through to 5° at 1° increments. The reason for the further decrease in total range of angle of attack is the same as the reason for the previous decrease, that being that for this flow velocity an increase in angle of attack above 5 degrees will result in incipient cavitation conditions. Following this the foil was again tested at random negative angles of attack in the same manner as the experimental data to prove the foils symmetrical nature. From these simulations as before coefficients for lift as well as drag and quarter chord pitching moments were extracted. Using the same process to obtain these performance criteria, pressure was integrated along the surface of the hydrofoil and the resulting vector split into components and substituted into the equations defined in the background theory. These results were then compared to experimental results from (Keerman 1956).

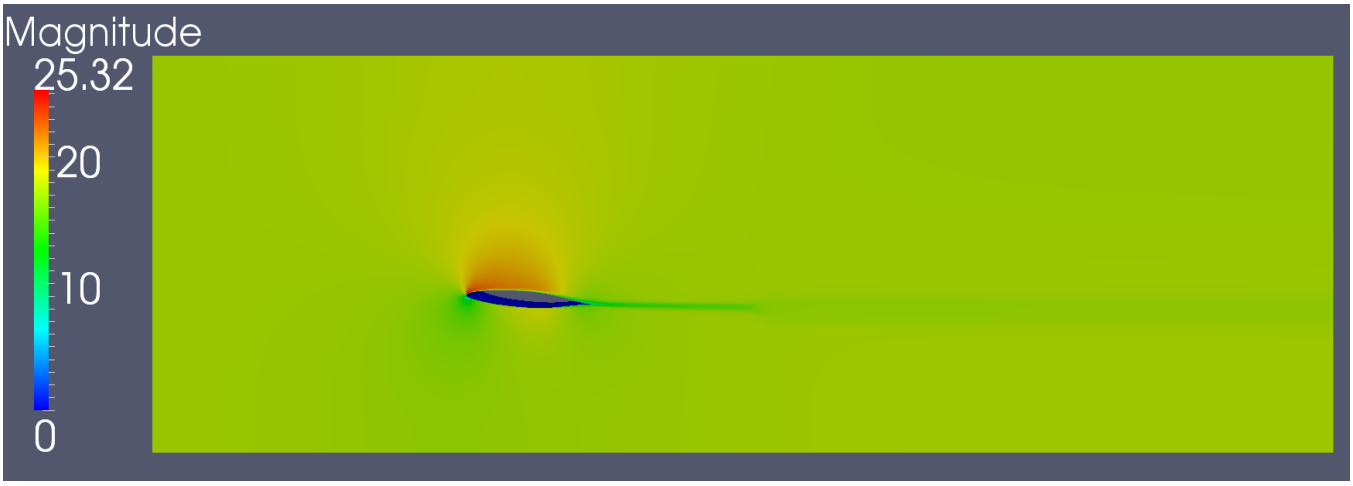

Figure 26: Velocity Field of NACA66-012 Foil at U =17.50 m/s and α = 5°

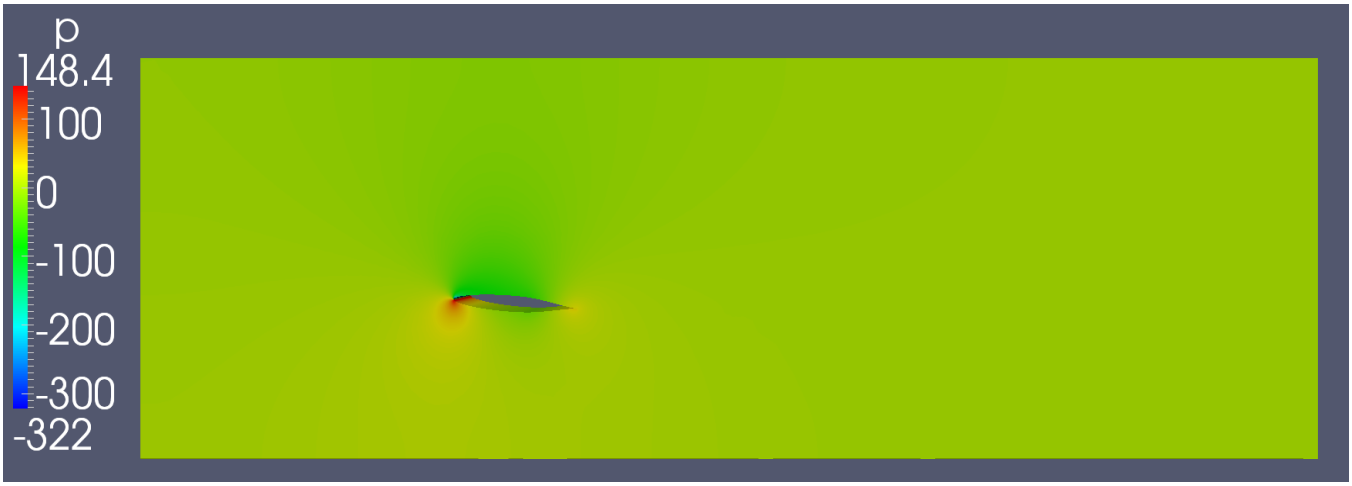

Figure 27: Pressure Field of NACA66-012 Foil at U =17.50 m/s and α = 5°

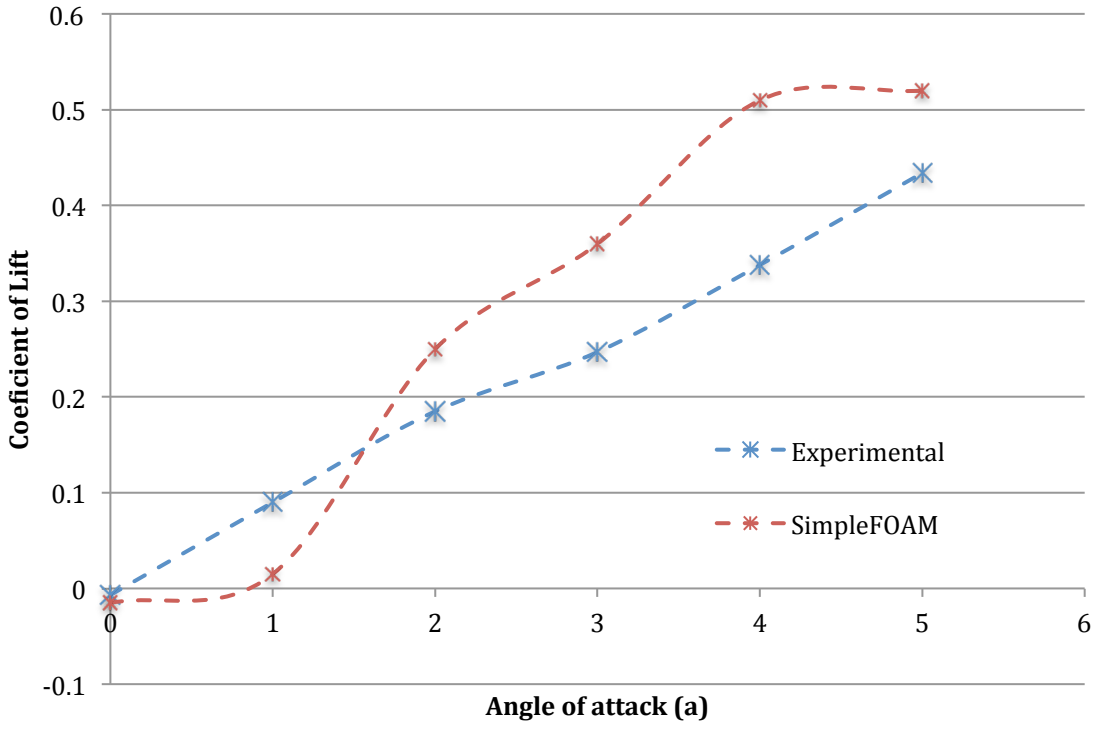

Figure 28: Comparison of Coefficients of Lift at U = 17.50 m/s

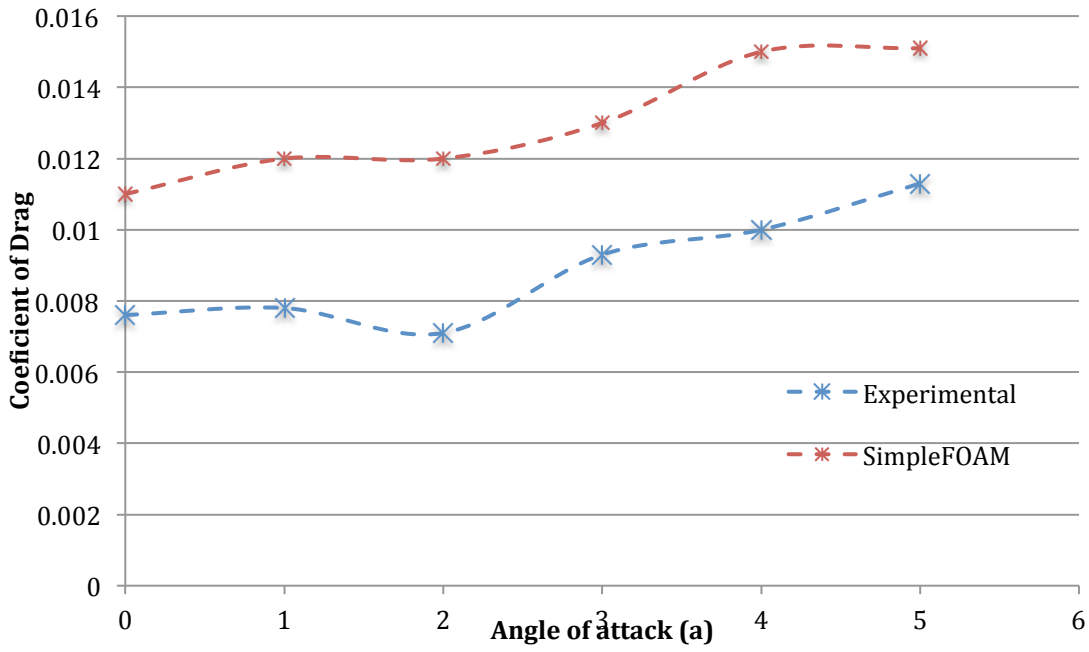

Figure 29: Comparison of Coefficients of Drag at U = 17.50 m/s

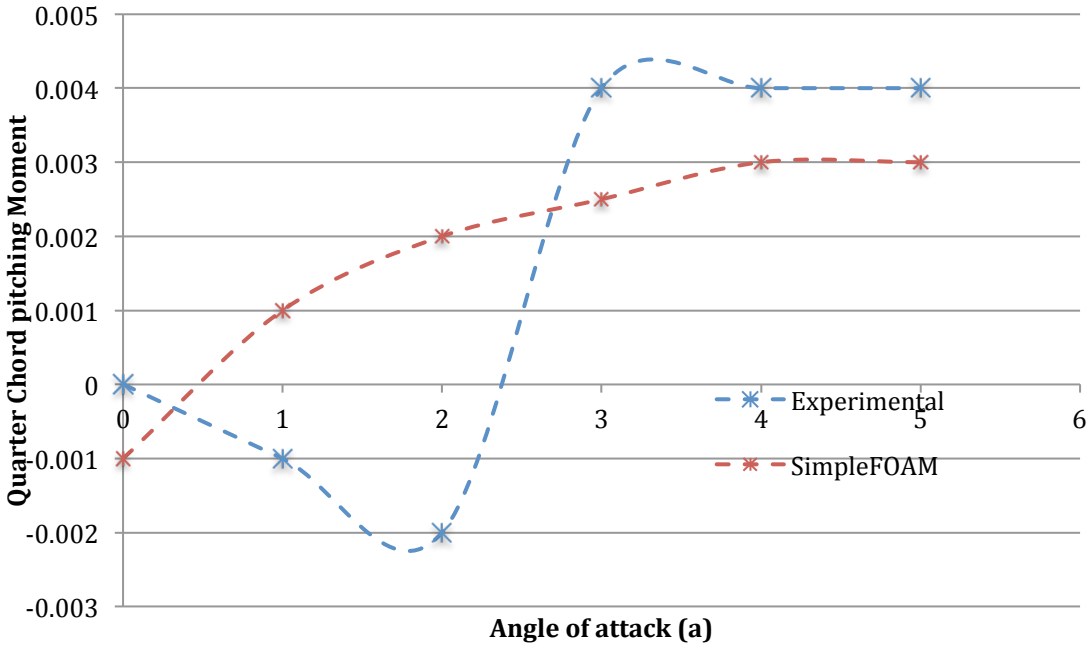

Figure 30: Comparison of Quarter Chord Pitching Moments at U = 17.50 m/s

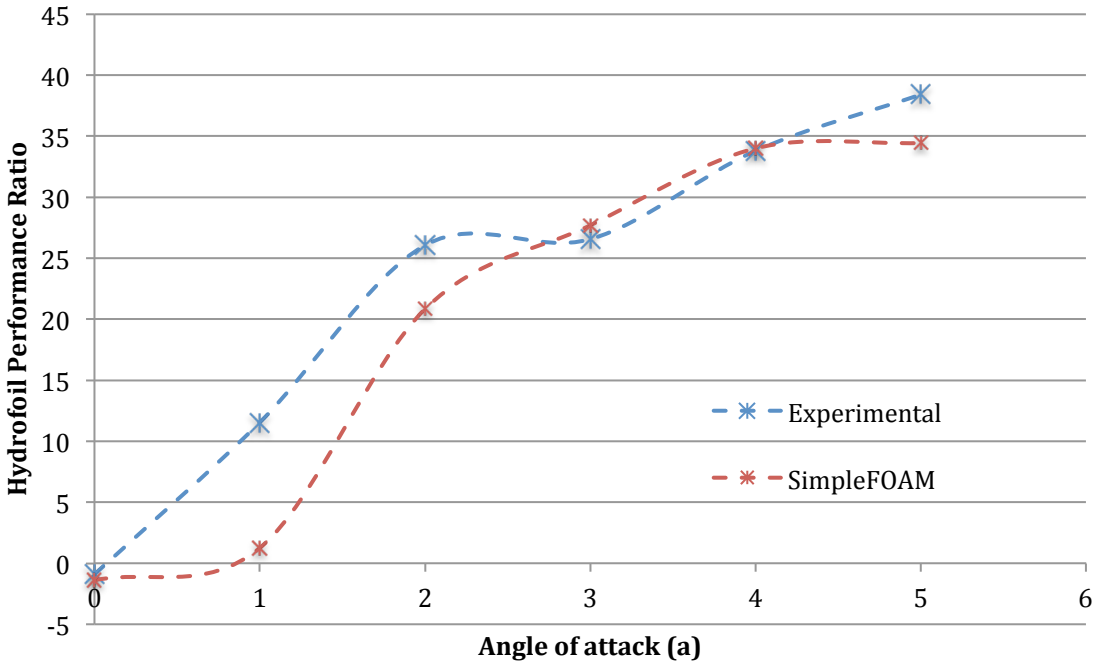

Figure 31: Performance Ratio of NACA66-012 Foil at U =17.50 m/s

[This Page Has Been Left Intentionally Blank]

4.0 Simulation of NACA66-012 Foil in Cavitating Flow Conditions

Simulation of cavitating flows was achieved in much a similar manner to the sub-cavitating cases with the exception of a number of differences. Unlike the sub-cavitating cases where a flow velocity was set and the angle of attack changed in the case of these simulations a flow velocity and angle of attack was set and the cavitation number was varied by adjusting the free stream pressure of the flow. In this case the angle of attack of the NACA66-012 foil was set at a constant 10° and the flow velocity set at 9.45 meters per second. Whilst the domain of the case was maintained, in order to accurately model the cavitation effects the resolution of the mesh was increased with an increase in the maximum allowable number of cells by 2 million. Additionally in the processing phase potentialFoam was no longer used to initialize the flows as this lead to unusual pressure distributions when running the simulation. In addition due to the incredibly high processing power requirements for running the chosen solver model interphaseChangeFoam turbulence modeling was removed and replaced with a laminar scheme in order to reduce the required CPU hours for running the case. This was implemented as to run these cases in a timely manner processing was outsourced to the iVEC supercomputing cluster at Murdoch which had a set limit of CPU hours available. In this simulation performance characteristics were recorded in the same manner as for the sub-cavitating cases for fluid flows with cavitation numbers ranging from 5.4 to 0.220.

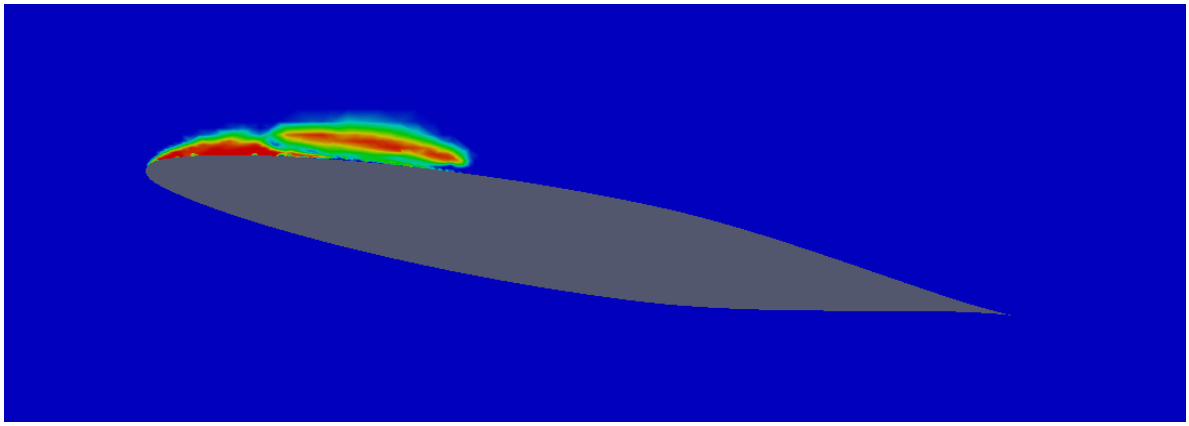

Figure 32: Close View Vapour Fraction at Cavitation Number k =1.518, U = 9.45 m/s and α = 10°

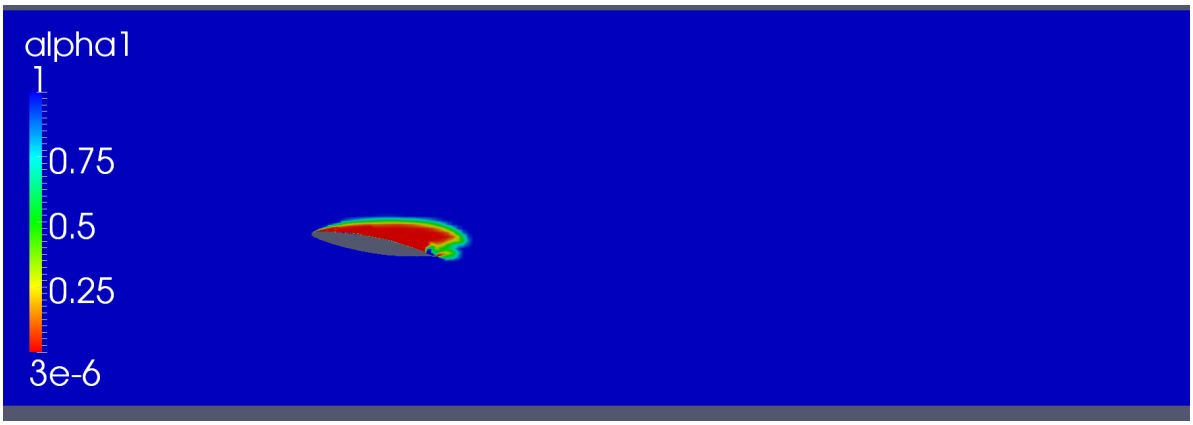

Figure 33: Vapour Fraction at Cavitation Number k =0.220, U = 9.45 m/s and α = 10°

Note from the above two figures it can be seen that an increase in the cavitation number of the system will result in a reduction of cavitation effects, generally a cavitation number above 3 is considered a non-cavitating flow. In the conditions tested it can be seen that for the cavitation number of k = 1.518 there is incipient level of cavitation behind the leading edge of the hydrofoil with vapor bubbles sheading from the surface of the hydrofoil. Note in the above figures the colors indicate the vapor fraction of the fluid with blue indicating a complete fluid and at the opposite end of the scale indicating complete vapor. In the case of the second figure where the cavitation number 0.220 it

can be seen that there is a fully developed vapor cavity formed on nearly the complete top surface of the hydrofoil.

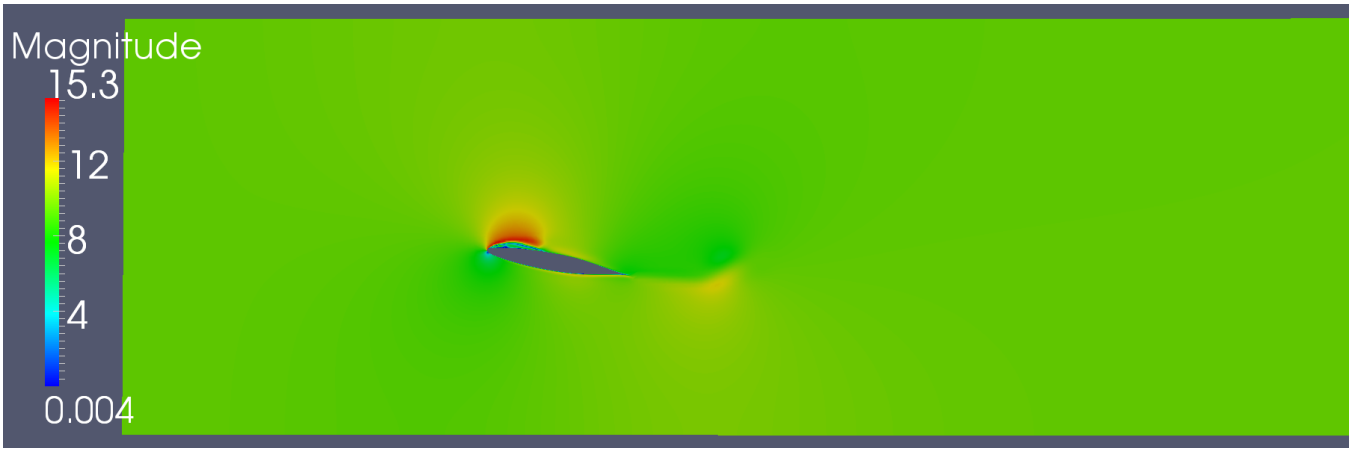

Figure 34: Velocity Magnitude Field at Cavitation Number k =1.518, U = 9.45 m/s and α = 10°

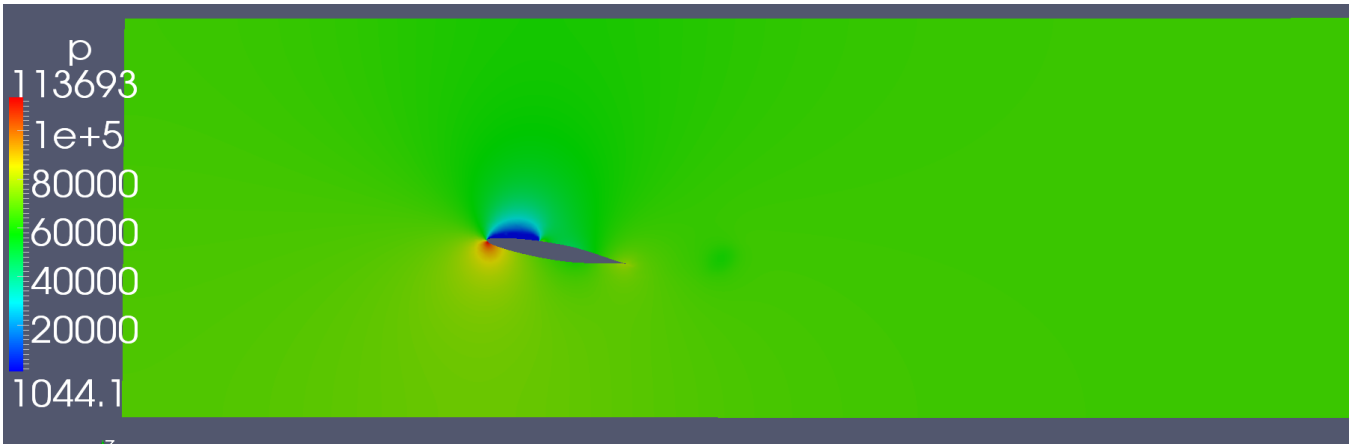

Figure 35: Pressure Magnitude Field at Cavitation Number k =1.518, U = 9.45 m/s and α = 10°

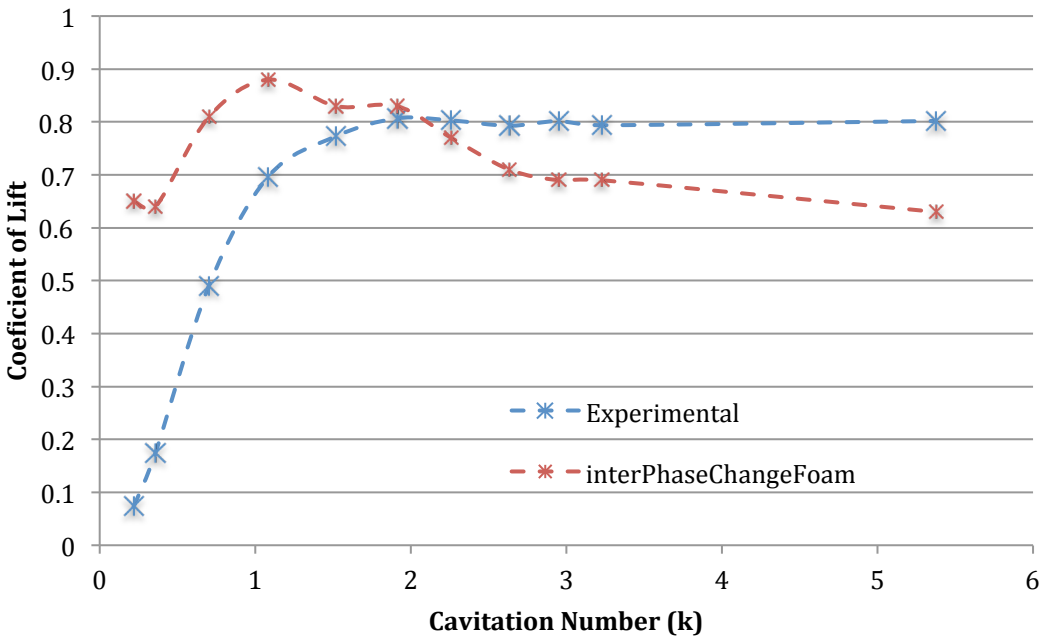

Figure 36: Comparison of Coefficients of Lift at U = 9.45 m/s and α = 10 °

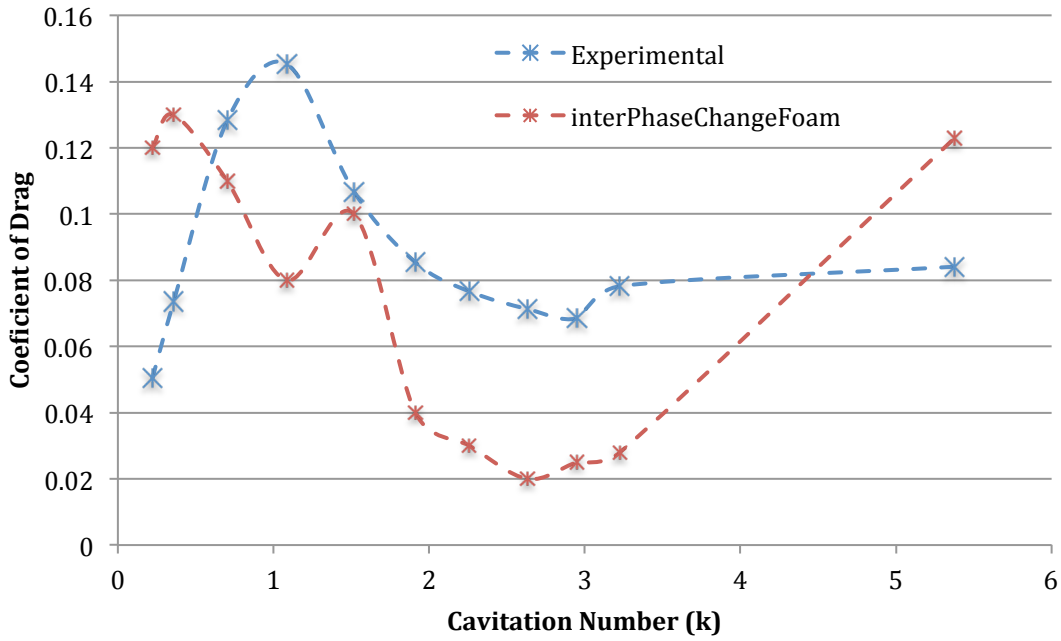

Figure 37: Comparison of Coefficients of Drag at U = 9.45 m/s and α = 10 °

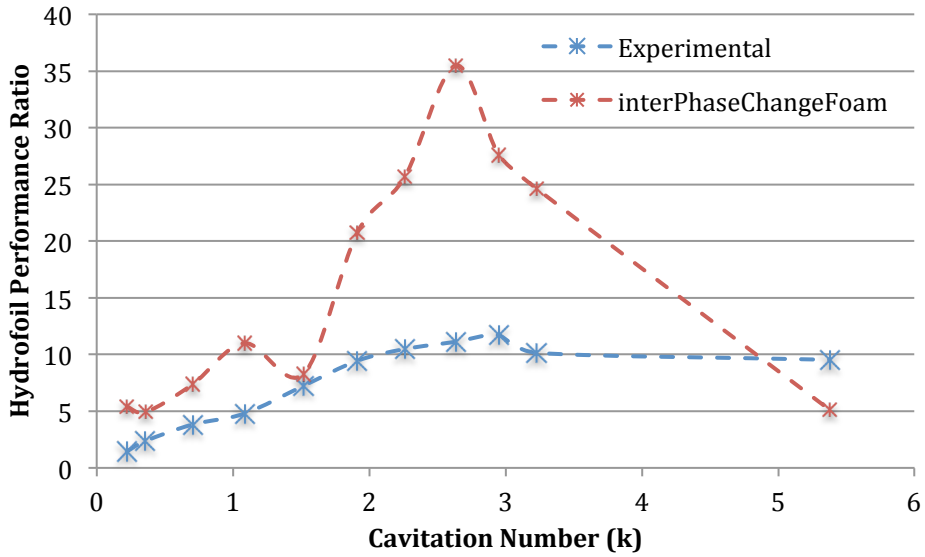

Figure 38: Comparison NACA66-012 Performance Ratios at U = 9.45 m/s and α = 10 °

[This Page Has Been Left Intentionally Blank]

5.0 Discussion

The results gained for the performance characteristics of the NACA66-012 hydrofoil in the sub-cavitating flow as described in chapter three of this report show that the performance predicted by the CFD techniques varied from that gained by Keerman in 1956 using experimental techniques.

For the first series of simulations using the simpleFoam model for sub-cavitating flow at 9.45 meters per second and angles of attack ranging from 0° to 13° there is a variation between the experimental and the CFD derived results. For the lift forces predicted at this flow velocity the CFD results follow the trend of the experimental results of a steady rise in force as the angle of attack is increased up to 11° where the lift forces plateau and then start to decrease as the foil reaches the critical angle of attack (also known as the stall angle) up to 13°. Whilst the trend is followed the actual force predicted by the CFD technique actually exceeds the experimental data by a fairly constant 10-15% percent. For the drag forces in this case it is a similar situation with the CFD data following the same trend as the experimental data but again over predicting the experienced force particularly at angles of attack of 10° or greater. The hydrofoil performance ratio at this flow velocity shows a high correlation between the two methods for angles 9° and greater but for angles less than this it tends to severely under predict the performance of the hydrofoil. For the quarter chord pitching moment the experienced forces follow a similar trend as the experimental result with a major exception occurring at angles greater than 10 degrees where the experimental data shows a rapid decrease to negative values whilst the CFD data shows the opposite of a rapid increase to greater positive values.

For the second series of simulations using the simpleFoam model for sub-cavitating flow at an increased velocity of 12.55 meters per second and a decreased series of angles of attack ranging from 0° to 11° as with the previous result there is a variation between the experimental and the CFD derived results. Also as with the previous data the lift and drag forces acing on the hydrofoil at this speed follow the trend of the

experimental data from Keerman quite closely with a tendency to over predict the expected forces by less than 20% in most cases. Also as with the previous case the hydrofoil performance ratio matches quite closely with the experimental data for angles of attack 9° or greater whilst below these angles it also tends to under predict the lift to drag ratio of the foil.

For the third and final series of simulations using the simpleFoam model for sub-cavitating flow at an increased velocity of 17.50 meters per second and a decreased series of angles of attack ranging from 0° to 5° unlike the previous two sets result there is a greater variation between the experimental and the CFD derived results. For the coefficient of lift for this simulation the CFD results show a far reduced force for angels of 0° and 1° then the trend crosses the experimental data and predicts lift forces far exceeding those predicted by Keerman for greater angles. For the drag forces calculated for these simulations the CFD data consistently predicts forces around 50% greater than the experimental data. For the hydrofoil performance ratio at this flow velocity the CFD data matches the experimental data quite closely for angles 2° and above however below this particularly at 1° the CFD data shows a performance far less than the experimental data.

The simulations of cavitating flows carried out at a constant speed of 9.45 meters per second and constant angle of attack of +10° showed much greater variance from the experimental data than those shown in the sub-cavitating cases. For lift forces greater than cavitation numbers of 1.5 the force calculated using CFD techniques were quite similar to the experimental data of Keerman however below this cavitation number the predicted lift forces far exceeded the experimental data. For the resultant drag forces between cavitation numbers of 0.7 and 4.5 the interPhaseChangeFoam model tended to predict forces lower than the experimental data whilst outside these cavitation numbers the forces tended to be greater than what would be expected. For the hydrofoil performance ratio in this flow there is a reasonable correlation for cavitation numbers less than 1.5 however above this point there is a rapid spike well above the experimental data followed by a rapid decline from just above a k value of 3.

There are a number of possible sources of error that must be considered, which potentially could have contributed to the variances between the experimental data and that from the CFD simulations.

Firstly in all cases of computational fluid dynamics the design and quality of the mesh plays an important role in the quality of the results produced. Whist it is desirable to have as fine a mesh as possible doing so will require increasing quantities of computational power to resolve a solution. For this reason it is important to strike a suitable balance between quality and efficiency. Additionally some fluid dynamics effects such as cavitation benefit from having a finer mesh specifically in the region where such effects occur. The mesh designed for the sub-cavitating flows had a limit of approximately 3.5 million cells with a relativity coarse domain mesh with a high level of refinement increasing in proximity of the foil with particular interest placed on the leading and trailing edges of the foil as these points are critical to predicting foil performance (Ofer 2008). For the cavitating flows the mesh limit was increased by 2 million cells to 5.5 million cells with particular interest placed on the surface behind the leading edge of the foil. Whilst these are large cell limits for such a simulation it is still likely that there would have been some effect on the results due to this.

For the sub-cavitating flows the use of the very basic simpleFoam solver model that does not allow for compressibility of the fluid could have contributed to the error in the results. Whist water at the pressures experienced has less than negligible compressibility this most basic of solvers is not an ideal solution as it does not account for a number of hydrodynamic effects. Additionally turbulence modelling on the surface of the hydrofoil using the RANS two-equation k-ω SST model could have also contributed. Whist RANS turbulence modelling is one of the least processor intensive model schemes it is known to produce poor results in comparison to a more advanced turbulence model such as LES and is this considered to be among “the best of the worst”.

In the case of the cavitating flow simulations there were also a number of possible sources of error. Firstly cavitation is a complex phenomenon and there are large variations in methods for modelling its effects such as models based on barotropic equations of state or like the interPhaseChangeFoam model used based on the transport equation of vapour fractions. The result of using different modelling methods is that some work only in specific styles of simulations and thus the selection of the most suitable model is important in producing accurate results. Additionally in order to save computational power in already computationally intensive simulations turbulence was modelled using a laminar model scheme, which could have also resulted in potential errors in the results.

Overall the results gained for the sub-cavitating flow simulations can actually be considered to have produced reasonable results for such a basic simulation. In the case of the cavitating simulations whilst the data shows larger than expected discrepancy's between the CFD and experimental data the results of the project can again be considered relatively good as stated by Gosset when using interPhaseChangeFoam which is considered OpenFOAM's best solver for hydrofoil cavitation results within an order of magnitude are acceptable.

In hindsight there are a number of changes that could have been applied to this project that could have resulted in procurement of better data. Whist it is acknowledged that OpenFOAM is a particularly powerful and versatile CFD package it has a especially steep learning curve with little documentation on the process of creating new and customised simulations. For this reason it is considered that greater levels of co-operation and communication between students using this package especially for the first half of the project period would offer substantial benefits. Secondly the simulations were set to rotate the hydrofoil at the midchord point when changing the angle of attack. This required recalculation of the axis of rotation of the quarter chord for each simulation. This proved to be a severe problem as the pitching moment is highly sensitive to the positioning of this axis with the slightest variation resulting in large discrepancy's of the quarter chord pitching moment.

6.0 Conclusions

The importance of computational fluid dynamics techniques in the development of hydrofoil design is becoming increasingly apparent as demand for larger and high performing hydrofoil craft meets the technological wall in hydrofoil design. CFD presents the potential for watercraft designers to increase design efficiency and reduce development costs.

This study attempts to validate the use of an open source CFD package, OpenFOAM to assess the performance characteristics of a hydrofoil in both sub-cavitating and fully cavitating flows and compare these to known performance characteristics for such a design obtained previously using experimental methods. A symmetrical NACA 66-012 section hydrofoil was selected and its performance characteristics including parameters such as lift and drag coefficients and quarter chord pitching moments were calculated for a range of flow velocity's and angles of attack in sub-cavitating flow and at a constant angle of attack with varying cavitation numbers in cavitating flows, following this the results were compared to the known data.

Results gained from the sub-cavitating simulations shows that the forces experienced on a hydrofoil could be predicted to within a consistent 10-15% variance from the experimental data published by Keerman in 1956. In the case of the cavitating flow simulations showed large variances of up to 75% between the experimental and the CFD data. Whilst this variance would be considered large for such work according to work published by Gosset in 2010 notes that for a simulation using the OpenFOAM solver model selected on a symmetrical hydrofoil that results within an order of magnitude are acceptable.

Thus the set objectives of this project were completed successfully as simulation of flows sub-cavitating through to fully developed cavitation were modelled for the NACA66-012 hydrofoil and the results were compared to experimental data and were

found to be within an acceptable level of agreement for the given software package used.

6.1 Recommendation for Future Works.

There are a number of recommendations that could be made for future work on this project including.

1. Increasing the range of flow velocities and angles of attack for both sub-cavitating and especially for cavitating flow regimens.
2. Using different solvers such as rhoSimpleFoam and cavitatingFoam and comparing the results gained both to the experimental data and those derived during this project.
3. Add supporting structure to the foil such as what would bee seen when attaching such a foil to a hydrofoil craft.
4. Add surface features or adjust the profile by using modifications such as fins or bumps such as those seen on objects such as golf balls tin order to see if the performance characteristics could be improved.
5. Simulate venting through the hydrofoil to see if the performance characteristics could be improved.
6. Simulate interaction of the hydrofoil near a free surface to inspect the effects of mixing on the performance of the foil.

7.0 References

1. R., Keerman. "Water Tunnel Tests of the Naca 66-012 Hydrofoil in Non Cavitatin and Cavitating Flows." Pasadena California: Department of Navy, Beauro of Ships, 1956.
2. Jamieson, J.J., W.E. Farris, and BOEING CO SEATTLE WASH ADVANCED MARINE SYSTEMS ORGANIZATION. *Hydrofoil Simulation Equations Study: Performance Criteria and Test Report for Hydrofoil Craft*. Defense Technical Information Center, 1966.
3. Versteeg H.K., Malalasekera W. *An Introduction to Computational Fluid Dynamics: The Finite Volume Method*. Longman Scientific & Technical, 1995.
4. Pike, J. "Hydrofoil Limitations." (2011). Published electronically 07/07/2011. http://www.globalsecurity.org/military/systems/ship/hydrofoil-limits.htm.
5. Gosset, A. Díaz Cásas, V. López Peña, F. "Evaluation of the Cavitatingfoam Solver for Low Mach Number Flow around a 2d Hydrofoil." (2010).
6. Schlichting, H., and K. Gersten. *Boundary-Layer Theory*. MacGraw-Hill, 2000.
7. Brennen, Christopher E. "Cavitation and Bubble Dynamics." (2003). http://caltechbook.library.caltech.edu/archive/00000001/00/chap1.htm.
8. Reynolds, Osborne. "On the Effect of Immersion on Screw Propellers." *Transactions of the Institute on Naval Architects* (march 27th 1874).
9. Franc, J.P., and J.M. Michel. Fundamentals of Cavitation. Kluwer Academic Publishers, 2006.
10. Savchenko, Yuriy N. "Supercavitation - Problems and Perspectives ", National Academy of Sciences, 2001.
11. Thom, A. "The Flow Past Circular Cylinders at Low Speeds." *Proceedings of the Royal Society of London. Series A, Containing Papers of a Mathematical and Physical Character* 141, no. 845 (September 1st 1933): 651-69.
12. Kawaguti, Mitutosi. "Numerical Solution of the Navier-Stokes Equations for the Flow around a Circular Cylinder at Reynolds Number 40." *Journal of the Physical Society of Japan* 8, no. 6 (1953): 747-57.

13. Land, Norman S. "Charachteristics of a Naca 66 S-209 Hydrofoil Section Hydrofoil at Several Depths ", edited by National advisory comittee for aeronautics. Langley Field Va, 1943.
14. Sheng Huang, Miao He, Chao Wang, Xin Chang. "Simulation of Cavitating Flow around a 2-D Hydrofoil." *J. Marine* 9 (June 6 2010): 63-16.
15. P. R. Spalart., "Strategies for turbulence modelling and simulations," *Boeing Commercial Airlines, P.O. Box 3707, Seattle, WA 98124, USA, International Journal of Heat and Fluid Flow,* 19 February, 2000
16. Land, Norman S. "Charachteristics of a Naca 66 S-209 Hydrofoil Section Hydrofoil at Several Depths ", edited by National advisory comittee for aeronautics. Langley Field Va, 1943.
17. Amromin, E., Kopriva, J., Arndt, R. & Wosnik, M. (2006), Hydrofoil drag reduction by partial cavitation, J. Fl. Eng. 128, 931-936.
18. Kjeldsen, M., Arndt, R. & Effertz, M. (2000), Spectral characteristics of sheet/cloud cavitation, J. Fl. Eng. 122, 481-487.
19. Aharon, Ofer. "Mit - 2.094 - Term Project - Hydrofoil Analysis Using Cfd." MIT, 2008.

Appendices

(See Attached Disk)